

AD _____

Award Number: DAMD17-01-2-0032

TITLE: Low Vision Research at The Schepens Eye Research Institute

PRINCIPAL INVESTIGATOR: Patricia A. D'Amore, Ph.D.

CONTRACTING ORGANIZATION: The Schepens Eye Research Institute
Boston, Massachusetts 02114

REPORT DATE: July 2002

TYPE OF REPORT: Annual

PREPARED FOR: U.S. Army Medical Research and Materiel Command
Fort Detrick, Maryland 21702-5012

DISTRIBUTION STATEMENT: Approved for Public Release;
Distribution Unlimited

The views, opinions and/or findings contained in this report are those of the author(s) and should not be construed as an official Department of the Army position, policy or decision unless so designated by other documentation.

20021024 075

REPORT DOCUMENTATION PAGE

*Form Approved
OMB No. 074-0188*

Public reporting burden for this collection of information is estimated to average 1 hour per response, including the time for reviewing instructions, searching existing data sources, gathering and maintaining the data needed, and completing and reviewing this collection of information. Send comments regarding this burden estimate or any other aspect of this collection of information, including suggestions for reducing this burden to Washington Headquarters Services, Directorate for Information Operations and Reports, 1215 Jefferson Davis Highway, Suite 1204, Arlington, VA 22202-4302, and to the Office of Management and Budget, Paperwork Reduction Project (0704-0188), Washington, DC 20503

1. AGENCY USE ONLY (Leave blank)	2. REPORT DATE	3. REPORT TYPE AND DATES COVERED	
	July 2002	Annual (1 Jul 01 - 30 Jun 02)	
4. TITLE AND SUBTITLE Low Vision Research at The Schepens Eye Research Institute			5. FUNDING NUMBERS DAMD17-01-2-0032
6. AUTHOR(S) Patricia A. D'Amore, Ph.D.			
7. PERFORMING ORGANIZATION NAME(S) AND ADDRESS(ES) The Schepens Eye Research Institute Boston, Massachusetts 02114			8. PERFORMING ORGANIZATION REPORT NUMBER
9. SPONSORING / MONITORING AGENCY NAME(S) AND ADDRESS(ES) U.S. Army Medical Research and Materiel Command Fort Detrick, Maryland 21702-5012			10. SPONSORING / MONITORING AGENCY REPORT NUMBER
11. SUPPLEMENTARY NOTES			
12a. DISTRIBUTION / AVAILABILITY STATEMENT Approved for Public Release; Distribution Unlimited			12b. DISTRIBUTION CODE
13. ABSTRACT (Maximum 200 Words) This research proposal, Low Vision at the Schepens Eye Research Institute, is a multi-disciplinary effort aimed at advancements in low vision research. Project 1, which focuses on dry eye complications of LASIK surgery, is in progress, having been delayed by the IRB process. Work on Project 2, ocular injury and inflammation, which has studied the role of FasL in corneal inflammation, has demonstrated that soluble FasL can block corneal inflammation induced by endotoxin. Project 3, which studies restoration of endothelial function of the damaged cornea, has assessed a variety of temperature sensitive polymers and growth factor for cornea endothelial cell growth. Project 4, which focuses on remote diagnosis of retinal damage, has obtained proof of principle for the optical plan for a portable prototype instrument to image retina for potential damage. Project 5, which studies regeneration of the damaged central nervous system, has defined the mechanism of lithium effects on retinal ganglion cell axon regeneration via Bc1-2 induction. Project 6, regulation of angiogenesis and the role of VEGF in adult, has developed transgenic mice that express a dominant negative VEGF Receptor 2 that will be used to generate mice in which VEGF signaling can be inducably blocked. Each of these efforts addresses critical and previously under-investigated elements that directly impact the health and vision of our military personnel.			
14. SUBJECT TERMS			15. NUMBER OF PAGES 45
			16. PRICE CODE
17. SECURITY CLASSIFICATION OF REPORT Unclassified	18. SECURITY CLASSIFICATION OF THIS PAGE Unclassified	19. SECURITY CLASSIFICATION OF ABSTRACT Unclassified	20. LIMITATION OF ABSTRACT Unlimited

NSN 7540-01-280-5500

Standard Form 298 (Rev. 2-89)
Prescribed by ANSI Std. Z39-18
298-102

Table of Contents

Cover.....	1
SF 298.....	2
Introduction.....	4
Project 1	
Body.....	4
Key Research Accomplishments.....	4
Reportable Outcomes.....	4
Conclusions.....	4
References.....	4
Appendices.....	5
Project 2	
Body.....	5
Key Research Accomplishments.....	5
Reportable Outcomes.....	5
Conclusions.....	5-7
References.....	7
Appendices.....	7-16
Project 3	
Body.....	17
Key Research Accomplishments.....	17
Reportable Outcomes.....	17
Conclusions.....	17-18
References.....	18
Appendices.....	18
Project 4	
Body.....	18-24
Key Research Accomplishments.....	24
Reportable Outcomes.....	24
Conclusions.....	24
References.....	24
Appendices.....	24-32
Project 5	
Body.....	33-34
Key Research Accomplishments.....	35
Reportable Outcomes.....	35
Conclusions.....	35
References.....	35-36
Appendices.....	36-42
Project 6	
Body.....	43-44
Key Research Accomplishments.....	44
Reportable Outcomes.....	44
Conclusions.....	45
References.....	45
Appendices.....	45

Introduction

The proposal, Low Vision Research at the Schepens Eye Research Institute (SERI), is a multi-disciplinary effort aimed at advancements in low vision research. The proposal encompasses six individual research projects each one led by one or two Principal Investigators. The proposal has direct military relevance in the areas of instrumentation, tactical advantage, and personnel readiness. In Year 1, the research includes investigations into ocular wound healing, ocular immunology, the control of angiogenesis, the regulation of neuroregeneration, the remote diagnoses of retinal damage, as well as a clinical study aimed at developing predictors of patient profiles for success with LASIK surgery. Each effort addresses the critical and previously under-studied elements that directly impact the vision of our military personnel.

Project 1. Dry Eye Complications of LASIK Surgery

Investigators: Drs. Dimitri Azar and Darlene Dartt

Body:

The administrative hold on this project was released on March 11, 2002 and the project was started at that time. We hired a study coordinator who developed charts to be filled out at the study evaluation visits and will coordinate the patient visits and archive the results. We also identified the medical personnel to perform the evaluations. They include an optometrist, a corneal fellow, and a research fellow. The research fellow optimized the techniques to be used to examine impressions of the cytology samples by histochemical staining and immunofluorescence microscopy. We next developed a recruitment brochure and have recruited one normal male subject to date who has completed the preoperative, 1 day, 3 day, and 1 week evaluations.

Key Research Accomplishments:

- Hired study coordinator
- Identified medical personnel to perform evaluations
- Developed recruitment brochure
- Recruited patient personnel

Reportable Outcomes:

None.

Conclusions:

None.

References:

None.

Appendices:

None.

Project 2. Ocular Injury and Inflammation

Investigator: Dr. Bruce Ksander

Body:

Our overall hypothesis of this project was that Fas Ligand (FasL) within the eye regulates the expression of innate immunity. Two forms of FasL have opposite regulatory roles: (i) cell-membrane bound FasL initiates innate immunity, and (ii) soluble FasL terminates innate immunity. Overall, our key research accomplishment was demonstrating that soluble FasL is effective in blocking corneal inflammation.

Key Research Accomplishments:

- membrane-only FasL initiates corneal inflammation via activation of infiltrating neutrophils.
- soluble FasL neither initiates corneal inflammation *in vivo*, nor activates neutrophils *in vitro*.
- wild-type FasL (membrane plus soluble) displays weaker corneal inflammation *in vivo* and intermediate activation of neutrophils *in vitro*.
- a mixture of soluble to membrane FasL (ratio of 1:1) blocks the development of corneal inflammation *in vivo*, and blocks the activation of neutrophils *in vitro* (as measured by the release of IL-1 beta).
- Soluble FasL is capable of blocking corneal inflammation induced by LPS.

Reportable Outcomes:

One manuscript in press (copy appended).

One manuscript in preparation.

Two abstracts (ARVO (the Association for Research in Vision and Ophthalmology) and FASEB (the Federation of American Societies for Experimental Biology))

Two oral presentations at ARVO and FASEB.

Drs. Meredith Gregory and Victor Perez worked on this project. Dr. Gregory was awarded the American Association of Immunologists Fellows Achievement Award for her research (awarded at FASEB). She also won the Cora Ver Hagen Prize (second place) for her research (awarded at ARVO). Dr. Perez won the New England Ophthalmologists Fellows Research Award for his research.

Conclusions:

The form of FasL is critical in determining its' function. The membrane form initiates innate inflammation and the soluble form terminates inflammation within the cornea. Our data imply

that the soluble form of FasL can be used to effectively block inflammation associated with bacterial keratitis.

There were four specific aims designed to test our hypothesis that Fas Ligand (FasL) within the eye regulates the expression of innate immunity. The results from these four specific aims are briefly summarized below.

Aim #1- Determine how the expression of different forms of Fas Ligand (FasL) expressed on corneal tissue alters activation of neutrophils. Our experimental results indicate (i) membrane-only FasL initiates corneal inflammation via activation of infiltrating neutrophils, (ii) soluble FasL neither initiates corneal inflammation *in vivo*, nor activates neutrophils *in vitro*, (iii) wild-type FasL (membrane plus soluble) displays weaker corneal inflammation *in vivo* and intermediate activation of neutrophils *in vitro*. *In vitro* activation of neutrophils was determined via IL-1 beta secretion.

We are currently examining different levels of membrane FasL in order to determine the “threshold” level of membrane FasL required to initiate corneal inflammation. There is a minimum level of mFasL required to initiate inflammation. We predict the minimum level within the cornea is significantly higher, as compared with the minimum level in a non-immune privileged site. Our current preliminary data supports this prediction. Moreover, we suspect the higher threshold for mFasL in the eye is due to the ocular environment, particularly aqueous humor. Our current experiments are directed at testing these predictions.

Aim #2- Determine if the addition of soluble FasL prevents the activation of neutrophils. Our experimental results indicate that (i) a 1:1 mixture of soluble to membrane FasL blocks the development of corneal inflammation *in vivo*, and (ii) the same mixture blocks the activation of neutrophils *in vitro* (as measured by the release of IL-1 beta).

The pro-inflammatory properties of mFasL requires that the eye, in “normal” situations, maintains a high ratio of soluble / membrane FasL. Our preliminary results suggest that wild-type FasL is actively cleaved at a higher rate within the ocular environment. Our next experiments will be directed at confirming these preliminary results and identifying the factor(s) that mediate the cleavage of mFasL into soluble.

Aim #3- Determine if soluble FasL prevents activation of neutrophils that are triggered via LPS and *not* via the Fas receptor. In the previous series of experiments we examined the ability of soluble FasL to block corneal inflammation that was induced by the expression of membrane FasL. While these experiments are important in determining the function of the different forms of FasL, they do not address whether sFasL can be used to block corneal inflammation that is triggered by pathogens. This is critical in proving sFasL is useful in clinical situations.

LPS is a component of the bacterial cell wall and induces a vigorous inflammatory response. Injection of LPS into the corneal stroma induces stromal keratitis that progresses to corneal neovascularization and scarring. In our experiments, we expressed sFasL within the corneal stroma one day prior to a stromal injection of LPS. As a control, we expressed the empty vector within the stroma. As expected, stromal keratitis developed in corneas that did not express sFasL

and progressed until central corneal scars developed with neovascularization. By contrast, corneas that expressed sFasL developed only a very slight and mild infiltrate that was gone within the first 48 hrs. All (100%) of the corneas were protected from corneal scarring and neovascularization. We conclude from these experiments that sFasL is capable of blocking corneal inflammation induced by LPS. This implies soluble FasL is effective in controlling inflammation associated with bacterial keratitis. Future experiments will directly test whether sFasL can prevent the development of destructive bacterial keratitis.

Aim #4- Determine if pre-exposure of neutrophils to soluble FasL prevents subsequent activation of neutrophils. These experiments are currently in progress. We are pre-treating neutrophils with sFasL and then stimulating them with either LPS, or mFasL. We predict that pre-treatment will reduce the release of pro-inflammatory cytokines by neutrophils.

References:

None.

Appendices:

Gregory, MS, Repp, AC, Holhbaum, AM, Saff, RR, Marshak-Rothstein, A, Ksander, BR. Membrane Fas Ligand Activates Innate Immunity and Terminates Ocular Immune Privilege. *The Journal of Immunology*, 2002 (in press).

Membrane Fas Ligand Activates Innate Immunity and Terminates Ocular Immune Privilege¹

Meredith S. Gregory,* Amanda C. Repp,* Andreas M. Holhbaum,[†] Rebecca R. Saff,[†] Ann Marshak-Rothstein,[†] and Bruce R. Ksander^{2*}

Q: A It has been proposed that the constitutive expression of Fas ligand (FasL) in the eye maintains immune privilege, in part through inducing apoptosis of infiltrating Fas⁺ T cells. However, the role of FasL in immune privilege remains controversial due to studies that indicate FasL is both pro- and anti-inflammatory. To elucidate the mechanism(s) by which FasL regulates immune privilege, we used an ocular tumor model and examined the individual roles of the membrane-bound and soluble form of FasL in regulating ocular inflammation. Following injection into the privileged eye, tumors expressing only soluble FasL failed to trigger inflammation and grew progressively. By contrast, tumors expressing only membrane FasL 1) initiated vigorous neutrophil-mediated inflammation, 2) terminated immune privilege, and 3) were completely rejected. Moreover, the rejection coincided with activation of both innate and adaptive immunity. Interestingly, a higher threshold level of membrane FasL on tumors is required to initiate inflammation within the immune privileged eye, as compared with nonprivileged sites. The higher threshold is due to the suppressive microenvironment found within aqueous humor that blocks membrane FasL activation of neutrophils. However, aqueous humor is unable to completely block the proinflammatory effects of tumor cells that express high levels of membrane FasL. In conclusion, our data indicate that the function of FasL on intraocular tumors is determined by the microenvironment in conjunction with the form and level of FasL expressed. *The Journal of Immunology*, 2002, 169: 0000–0000.

Fas ligand (FasL)³ is a 40-kDa type II transmembrane protein of the TNF family that induces apoptotic cell death of susceptible cells expressing the Fas receptor (1). Whereas the Fas receptor is ubiquitously expressed on multiple cell types, FasL expression is restricted primarily to activated T cells, NK cells, and immune privileged sites such as the testis, brain, placenta, and eye (2). The Fas-FasL system is fundamental in maintaining homeostasis of the immune system. In addition, the constitutive expression of FasL within the eye is thought to contribute to the maintenance of the immune privileged environment (3).

The strict regulation of inflammatory reactions within the eye is vital in maintaining both anatomical integrity and visual function. Left unregulated, inflammation within the eye may lead to extensive ocular damage, resulting in impaired vision. Studies have demonstrated that the Fas-FasL system plays a pivotal role in preventing inflammation within the eye by triggering apoptosis of invading Fas-positive inflammatory cells, thus maintaining the immune privileged environment (3).

Despite the substantial evidence supporting the immunoprotective role for FasL within the eye, applying this phenomenon to the

field of transplantation using nonocular tissues has led to conflicting results (4–8). Lau et al. (5) reported that myoblasts transfected with FasL protected islet allografts from immune-mediated rejection. By contrast, Kang et al. (6) reported that FasL expression on pancreatic islets triggered neutrophil infiltration and graft rejection. Taken together, these studies indicated that FasL could either be immunoprotective, or immunodestructive. The eventual outcome may depend on the level of FasL expression and/or the moderating effects of the local microenvironment.

Recently, data from Chen et al. (9) indicated that the cytokine milieu within the eye antagonized the immunodestructive capacity of FasL-expressing tumors. FasL⁺ colon carcinoma cells (CT-26) were rejected if injected s.c. in the flank (a nonprivileged site). By contrast, when these same tumor cells were injected into the anterior chamber (AC) of the eye, they experienced immune privilege and grew progressively. Their results suggested that aqueous humor, the fluid within the AC, blocked FasL-induced inflammation, resulting in progressive tumor growth. These data support the idea that the local environment determines whether FasL is either immunoprotective or immunodestructive.

We sought to determine whether the form and/or level of FasL expressed within the ocular environment could modify immune privilege. FasL is a type II transmembrane protein (mFasL) that can be cleaved by specific metalloproteinases to release a soluble form of the protein (sFasL) (10–12). Because sFasL has been shown to antagonize the functional activity of mFasL (13, 14), cleavage serves to both reduce the level of mFasL and produce a natural antagonist. Therefore, the overall impact of FasL expression is likely to depend on the balance between the relative levels of mFasL and sFasL. To test this premise, tumor cells expressing wild-type (wtFasL), mFasL, or sFasL were evaluated for their ability to induce ocular inflammation. We found that although neither sFasL nor wtFasL could perturb the immune privilege status of the eye, tumor cells that expressed mFasL terminated ocular immune privilege and induced a potent neutrophil-mediated inflammatory

*Schepens Eye Research Institute, Department of Ophthalmology, Harvard Medical School, Boston, MA 02114; and [†]Department of Microbiology, Boston University School of Medicine, Boston, MA 02118

Received for publication December 3, 2001. Accepted for publication June 24, 2002.

The costs of publication of this article were defrayed in part by the payment of page charges. This article must therefore be hereby marked *advertisement* in accordance with 18 U.S.C. Section 1734 solely to indicate this fact.

¹This work was supported by National Institutes of Health Grants T32-EY07145 (to M.S.G.), F32-EY13664 (to M.S.G.), GM-58724 (to A.M.R.), T32-CA64070 (to A.M.H.), RO1-EY08122 (to B.R.K.), and Leukemia Society Grant LSA-6146 (to A.M.R.).

²Address correspondence and reprint requests to Dr. Bruce R. Ksander, Schepens Eye Research Institute, 20 Staniford Street, Boston, MA 02114. E-mail address: ksander@vision.eri.harvard.edu

³Abbreviations used in this paper: L5, L5178Y-R T lymphoma cells; FasL, Fas ligand; mFasL, membrane FasL; sFasL, soluble FasL; wtFasL, wild-type FasL; neo, no FasL; AC, anterior chamber; AqH, aqueous humor; MIP-2, macrophage-inflammatory protein-2.

response. Interestingly, we determined that the termination of immune privilege was dependent on the level of mFasL expressed on the tumor cell surface, by demonstrating that only tumor cells that expressed high levels of mFasL were capable of inducing an inflammatory response potent enough to terminate immune privilege. Furthermore, the suppressive microenvironment of aqueous humor could not block the proinflammatory effects of tumor cells expressing high levels of mFasL. Another intriguing finding was that termination of immune privilege and ocular inflammation led to the induction of a tumor-specific adaptive immune response. Taken together, our data demonstrate that both the form and level of FasL expressed within the suppressive microenvironment of the eye are critical in determining the immune privileged status of the eye.

Materials and Methods

Animals

Adult female DBA/2, C3H/HeJ, and C3.MRL-Fas^{lpr} mice (6–8 wk) and adult male and female SCID/beige mice were purchased from Taconic Farms (Germantown, NY). Aqueous humor was obtained from adult female New Zealand White albino rabbits purchased from Millbrook Breeding Labs (Amherst, MA). All animals were treated according to the Association for Research in Vision and Ophthalmology Resolution on the Use of Animals in Research.

Aqueous humor (AqH)

AqH was obtained as previously described (15) from the ocular AC by paracentesis through a 27-gauge perfusion set (Fisher Scientific, Pittsburgh, PA) into siliconized microfuge tubes. The aqueous humor was used immediately or transiently acidified according to the following standard procedure (16). Approximately 5 µl 1 N HCl (Sigma, St. Louis, MO) was added to 100 µl AqH, bringing the pH up to 2. The acidified sample was left for 1 h at 4°C. Renutralization of the acidified sample was conducted by adding a 1:1 mixture of 1 N NaOH (Sigma) and 1 M HEPES (Life Technologies, Gaithersburg, MD) (10 µl/100 µl AqH) to return the pH to 7.3. Both fresh and transiently acidified AqH were added to neutrophil cultures as described below.

Tumor cell lines

L5178Y-R tumors expressing no FasL (L5-neo), wtFasL (L5-wtFasL), sFasL (L5-sFasL), or mFasL (L5-mFasL) were produced as previously described (13). Tumor cells were grown in suspension cultures in RPMI 1640 (Life Technologies) supplemented with 10% heat-inactivated FCS (HyClone, Logan, UT), 0.01 M HEPES buffer, 2.0 mM glutamine (Life Technologies), 100 U/ml penicillin G sodium (Life Technologies), 100 g/ml streptomycin sulfate (Life Technologies), 2-ME (1×10^{-5} M; Sigma), and 800 µg/ml Geneticin (Life Technologies).

Evaluation of FasL expression by flow cytometry

Flow cytometry was used to assess surface expression of FasL on L5178Y-R tumor cells expressing no FasL, wtFasL, mFasL^{low}, or mFasL^{high}. Tumor cells (1×10^6 cells) were stained with PE-conjugated anti-mouse FasL (MFL3; BD PharMingen, San Diego, CA) in 50 µl of staining buffer (1× PBS, 1.0% BSA, 0.02% NaNO₃) for 30 min on ice and washed three times with staining buffer. Cells were resuspended in 1× PBS and then analyzed on a FACScan flow cytometer (BD Biosciences, San Jose, CA), and the data were analyzed using CELLQuest software (BD Biosciences).

AC tumor inoculation and growth

L5 cells were washed in HBSS and resuspended in HBSS for inoculations. Using a quantitative technique that has been described previously, 2×10^3 cells in 3 µl were injected into the AC of DBA/2, C3H/HeJ, C3.MRL-Fas^{lpr}, or SCID/beige mouse eyes (17). Slit lamp examination was used daily to determine the percentage of the AC occupied by tumor cells. Tumor growth and ensuing inflammation were also examined histologically. Tumor-containing eyes were enucleated, fixed in 10% paraformaldehyde, embedded in paraffin, sectioned, and stained with H&E.

Subcutaneous tumor inoculation and growth

L5 cells (2×10^6 cells) were washed with HBSS and injected s.c. into the rear flanks of syngeneic DBA/2 mice (13). Tumor growth was followed for up to 3 wk by caliper measurements of perpendicular diameters.

Preparation of neutrophils

One milliliter of 9% casein solution (w/v in 0.9% saline) was injected into the peritoneal cavity of DBA/2 mice. A repeat injection was given 24 h later. Three hours after the second injection, the mice were euthanized, and the peritoneal cavity was washed twice with 5 ml of 1× PBS plus 0.02% EDTA. Cells from the peritoneal fluid were pooled from 4–5 mice and washed three times with 1× PBS. One milliliter of the cell suspension ($3\text{--}5 \times 10^7/\text{ml}$) was added to 9 ml of Percoll gradient solution (10 ml sterile 10× PBS plus 90 ml sterile Percoll (Pharmacia Biotech, Piscataway, NJ)). The mixture was ultracentrifuged for 20 min at 60,650 × g. The polymorphonuclear neutrophils were collected from the second opaque layer, washed with PBS, and checked for purity and viability. The purity of murine neutrophil preparations was determined by cytospin to be 98% neutrophils. The neutrophils were maintained in serum-free medium (RPMI 1640 supplemented with 0.01 M HEPES buffer, 1 mM sodium pyruvate (Life Technologies), 1 mM nonessential amino acids (Life Technologies), 100 U/ml penicillin G sodium, 100 g/ml streptomycin sulfate, 1 mg/ml BSA (Sigma), 50 mM 2-ME, and 1/500 diluted ITS plus 1 liquid AQ:B culture supplement (Sigma)).

Cytokine determinations

Murine neutrophils (300,000 cells/well) were incubated in a 24-well plate (Falcon; NJ) with serum free medium alone, or L5 tumor cells (300,000 cells/well) expressing either: 1) no FasL, 2) wtFasL, 3) sFasL, or 4) mFasL. The total volume was 1 ml of medium per well. For a positive control, neutrophils were incubated with 1 µg/ml LPS (SIGMA). In experiments that use aqueous humor (AqH), murine neutrophils (60,000 cells/well) were added to a 96-well, U-bottom plate (Falcon; BD Biosciences) with serum-free medium, 50% fresh AqH, or 50% transiently acidified AqH. The neutrophils were incubated in the presence or absence of L5 tumor cells (120,000 cells/well) expressing 1) no FasL, 2) wtFasL, or 3) mFasL. The total volume was 200 µl medium per well. For a positive control, neutrophils were incubated with 1 µg/ml LPS (Sigma).

For both culture systems, neutrophils and tumor cells were cultured together for 18 h at 37°C and 5% CO₂. At the end of the culture period, the plates were centrifuged at 500 × g for 5 min, and 50 µl of supernatant were harvested from triplicate cultures. The concentration of IL-1β and macrophage-inflammatory protein-2 (MIP-2) was measured using the Quantikine M Mouse Immunoassay kit according to the manufacturer's protocol (R&D Systems, Minneapolis, MN).

Assay for protective antitumor immunity

DBA/2 mice that had been injected with 2×10^3 L5-mFasL cells into the AC and had rejected the tumor were subsequently challenged (40 days after the initial AC injection) with a s.c. challenge of 2×10^5 L5-neo cells in the flank. Tumor growth was determined by measuring tumor diameter every two days with calipers.

Results

Expression of FasL on L5178Y-R lymphoma cells

The first series of experiments were designed to determine whether the form of FasL expressed on tumor cells altered their ability to experience ocular immune privilege. L5 tumor cells were transfected with four FasL cDNAs: 1) wild-type FasL; 2) mFasL; 3) sFasL, or 4) no FasL (empty vector; L5-neo). These tumor cells were characterized previously (13). Briefly, soluble FasL was detected in supernatants from L5-sFasL and L5-wtFasL cells, but not in supernatants from L5-mFasL cells. L5-sFasL cells secreted significantly more sFasL than L5-wtFasL cells. L5-mFasL cells expressed a 5- to 10-fold higher level of mFasL, as compared with L5-wtFasL cells (Fig. 1A). The lower level on L5-wtFasL cells was due, at least in part, to the cleavage of mFasL by matrix metalloproteinase enzymes, because addition of the metalloproteinase inhibitor KB8301 increased the amount of membrane FasL on L5-wtFasL cells (data not shown).

L5178Y-R lymphoma cells expressing mFasL trigger rejection of ocular tumors

Tumor cells were injected into syngeneic DBA/2 mice at either 1) a s.c. site in the flank (nonprivileged site) or 2) the AC of the eye (immune-privileged site). Tumor diameter was measured at regular

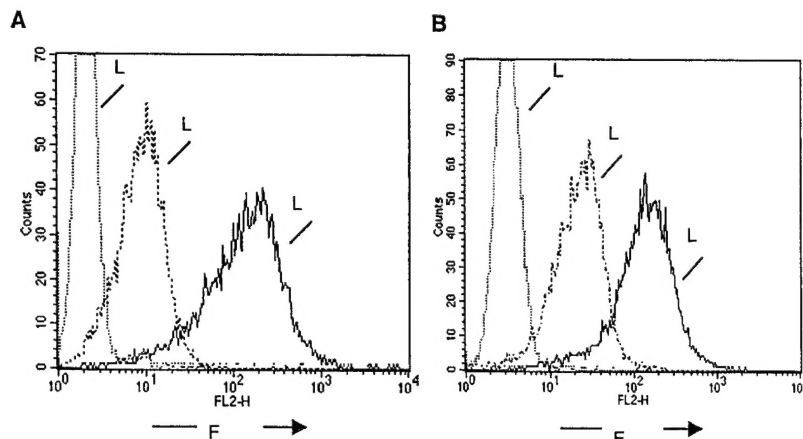


FIGURE 1. Characterization of FasL-expressing L5178Y-R lymphoma cell lines. L5-transfected tumor cells were stained with the anti-FasL mAb MF13 and analyzed by flow cytometry. *A*, The level of mFasL was compared among wtFasL, mFasL, and the negative control (L5-neo). *B*, The level of mFasL was compared among tumor cell clones that expressed no (L5-neo), low (L5-mFasL^{low}), and high (L5-mFasL) levels of mFasL. FL1-H, Fluorescence.

intervals and was used to assess s.c. tumor growth (Fig. 2), whereas histological analysis and survival was used to assess tumor growth within the AC of the eye (Fig. 3). As a positive control, L5-neo (FasL negative) tumors grew progressively in both the AC and s.c. sites, indicating that in the absence of FasL, the L5 tumors alone are not immunogenic (Fig. 2 and Fig. 3A). By definition, a tumor benefits from immune privilege within the AC if the tumor grows progressively within the eye but is rejected from the nonprivileged s.c. site. L5-wtFasL cells were rejected from the s.c. site (Fig. 2), but experienced immune privilege within the eye and 100% of the mice succumbed to progressive tumor growth (Fig. 3A). This same result was observed and reported by Chen et al. (9) and supports the hypothesis that wtFasL in the ocular environment contributes to immune privilege. Interestingly, tumors that expressed sFasL grew progressively in both s.c. and AC sites, displaying a growth pattern indistinguishable from L5-neo tumors (Figs. 2 and 3, *B–D*). Taken together, these data indicate that tumor cells expressing wtFasL experience immune privilege within the eye and grow progressively. In addition, tumor cells expressing sFasL fail to induce an antitumor inflammatory response in both nonprivileged and privileged sites.

L5-mFasL cells were rejected from the s.c. site (Fig. 2), but to our surprise, L5-mFasL cells experienced no immune privilege within the AC of the eye; tumors were rejected completely and all mice survived indefinitely (Fig. 3A). Tumor rejection within the

eye was examined histologically by comparing rejecting L5-mFasL tumors (Fig. 3, *E–G*) with progressively growing L5-neo tumors (Fig. 3, *B–D*). Three days after injection into the AC, L5-neo and L5-mFasL tumors were present within the anterior angle. By day 6 postinoculation the L5-neo tumors were growing progressively and by day 11 had filled 100% of the AC. By contrast, tumor regression and fibrosis was observed in the AC of mice injected with L5-mFasL cells on days 6 and 11 postinoculation. Complete rejection of mFasL-expressing tumors was observed by day 32 and resulted in phthisis of the tumor-containing eye. Phthisis typically occurs following an intense inflammatory response leading to nonspecific destruction of normal ocular tissue (18). Thus, L5-mFasL cells, but not L5-wtFasL cells, break through the immune privileged status of the eye.

mFasL alone stimulates ocular inflammation

Experiments from other laboratories found that rejection of non-ocular tumors expressing FasL coincided with infiltration of neutrophils (9, 13). To determine whether neutrophil infiltration coincided with rejection of tumors from the anterior chamber of the eye, histological analysis of the L5 derivatives was performed 9 days postinoculation. Tumor cells expressing no FasL (Fig. 4A) or L5-sFasL (Fig. 4B) grew to fill the AC with solid tumor, and there was no evidence of inflammatory infiltrate. By contrast, tumor regression was observed in mice that received inoculation of L5-mFasL cells (Fig. 4C). Furthermore, this regression was associated with an intense inflammatory response characterized by neutrophils present in both the cornea and AC (Fig. 4D). These results demonstrate that neutrophil infiltration coincides with rejection of L5-mFasL tumors in the eye.

L5178Y-R lymphoma cells expressing mFasL trigger neutrophil production of both MIP-2 and IL-1 β

Following recruitment to the site of inflammation, neutrophils play two major roles: 1) eradication of cellular debris through phagocytosis and release of hydrolytic enzymes and reactive oxygen products; and 2) recruitment and activation of additional neutrophils and other inflammatory cells through the production of proinflammatory cytokines and chemokines (19, 20). To determine whether L5-mFasL tumor cells could directly activate neutrophils to secrete the chemokine MIP-2 and proinflammatory cytokine IL-1 β , casein-elicited neutrophils were incubated (*in vitro*) with the L5 derivatives. Neutrophils were obtained from 1) DBA/2, 2) C3.MRL-Fas^{lpr}, or 3) C3H/HeJ mice. Cells from C3.MRL-Fas^{lpr} mice do not express functional Fas receptors and were used to demonstrate that cytokine secretion from neutrophils was triggered by the Fas receptor. The results were identical when neutrophils

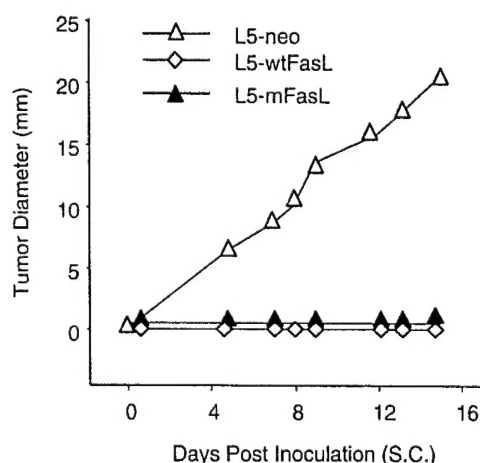


FIGURE 2. L5-wtFasL and L5-mFasL tumor cells are rejected following s.c. inoculation. DBA/2 mice received s.c. inoculations of 1×10^6 L5-neo, L5-wtFasL, or L5-mFasL cells. Tumor diameter was used to assess tumor growth and rejection. $n = 2$ (L5-neo), $n = 5$ (L5-wtFasL), and $n = 8$ (L5-mFasL).

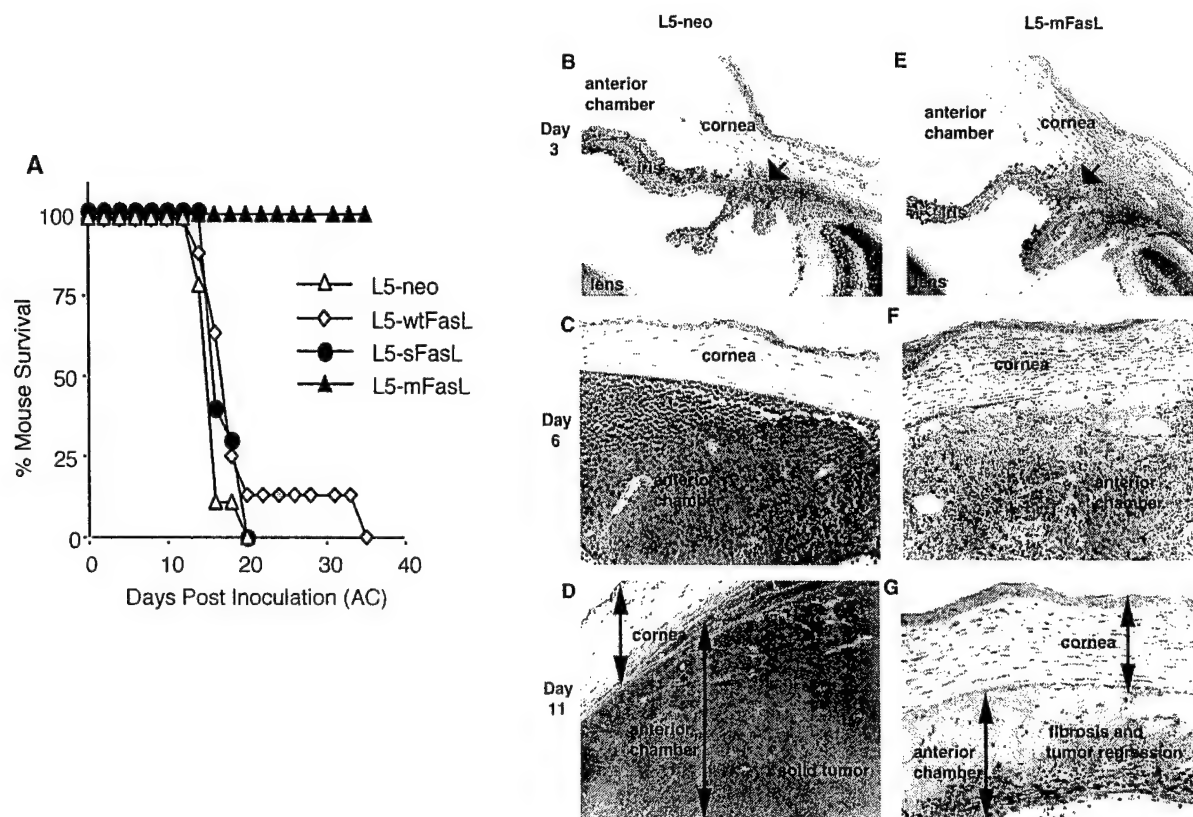


FIGURE 3. Tumor transfectants expressing mFasL are rejected following AC inoculation resulting in 100% survival. DBA/2 mice received AC inoculations of 2×10^3 L5-neo, L5-wtFasL, L5-sFasL, or L5-mFasL cells. Mouse survival was monitored daily (*A*) and histological analysis was performed at 3 days (*B* and *E*), 6 days (*C* and *F*), and 11 days (*D* and *G*) post-AC inoculation of either L5-neo or L5-mFasL tumor cells. Survival data were pooled from two independent experiments ($n = 8-10$ for each group). Magnification, $\times 20$; double-headed arrow, tumor cells.

were used from either DBA/2 or C3H/HeJ mice (data from DBA/2 mice not shown).

Interestingly, L5-mFasL cells stimulated Fas⁺ neutrophils to secrete significant amounts of MIP-2 (11.0 ± 0.4 pg/ml) and IL-1 β (20.0 ± 4.6 pg/ml), whereas L5-sFasL cells were unable to stimulate Fas⁺ neutrophils to secrete either MIP-2 or IL-1 β (Fig. 5). wtFasL-stimulated neutrophils secrete a small amount of both MIP-2 and IL-1 β . These data demonstrate that mFasL, but not sFasL, is capable of directly activating neutrophils to secrete both MIP-2 and IL-1 β .

L5-mFasL tumor cells stimulated production of both MIP-2 and IL-1 β only in neutrophils that expressed functional Fas receptors (MIP-2: 11.0 ± 0.4 pg/ml C3H vs 0 pg/ml MRL^{lpr}) (IL-1 β : 20.0 ± 4.6 pg/ml C3H vs 0 pg/ml MRL^{lpr}). As a positive control, LPS (a FasR-independent activator) stimulated production of both MIP-2 and IL-1 β equally well in neutrophils with and without functional FasR. Taken together, these data confirm that: 1) mFasL is capable of directly activating neutrophils; and 2) this activation is dependent on a functional Fas-FasL system.

AqH inhibits neutrophil production of IL-1 β

Previous studies by Chen et al. (9) demonstrated that the microenvironment of the eye, not the amount of FasL, determines whether wtFasL on tumor cells will activate neutrophils. However, these studies did not address the role of the form of FasL expressed on the tumor cells. To determine whether the microenvironment of the eye, particularly TGF- β , inhibits the production of IL-1 β by neutrophils stimulated with tumor cells expressing mFasL, casein-elicited neutrophils and L5 derivatives were incubated (*in vitro*) in the presence or absence of 50% AqH.

AqH contains many immunosuppressive factors that contribute to the immunosuppressive environment of the eye (21). However, only TGF- β has been shown to directly inhibit FasL activation of neutrophils (9). Whereas TGF- β is expressed at high levels in the AqH, the predominant form in fresh unperturbed AqH is latent

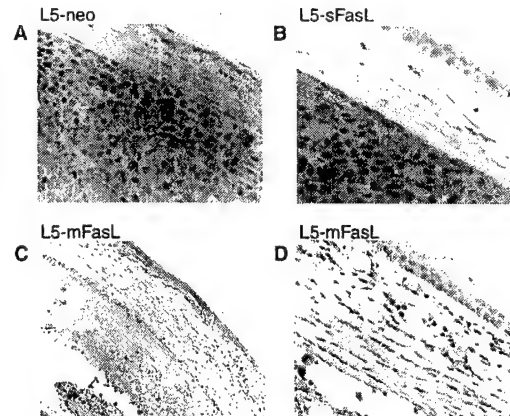
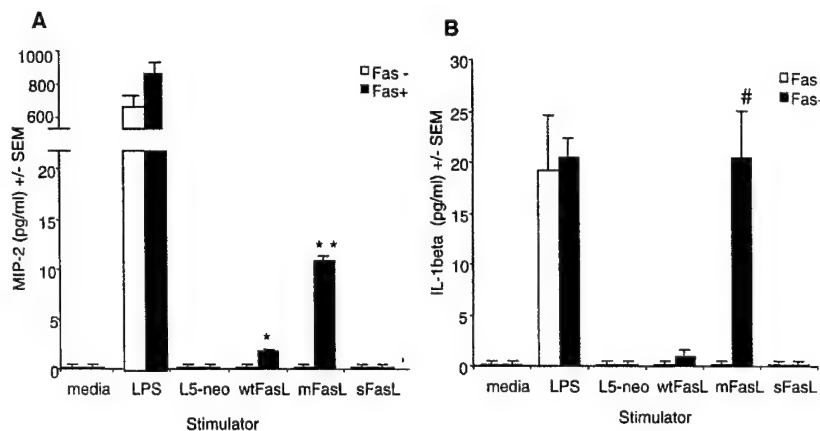


FIGURE 4. L5-mFasL cells trigger an inflammatory response characterized by neutrophil infiltration and tumor regression. DBA/2 mice received anterior chamber inoculations of 2×10^3 L5-neo, L5-sFasL, or L5-mFasL cells. Histological analysis of the L5 derivatives was performed at 9 days postinoculation. Progressive tumor growth and lack of inflammation was observed in both L5-neo (*A*) and L5-sFasL (*B*) tumors. In contrast, tumor regression and fibrosis (*C*) and neutrophil infiltration in both the cornea and anterior chamber was observed in mice that received L5-mFasL cells (*D*). Magnification: *A*, *B*, and *D*, $\times 60$; *C*, $\times 20$.

FIGURE 5. L5-mFasL cells stimulate Fas⁺ neutrophils to produce both MIP-2 and IL-1 β . Neutrophils (3×10^5 cells/well) were isolated from either Fas⁺ mice (C3H/HeJ), or Fas⁻ mice (C3.MRL-Fas^{lp}) and incubated with equal numbers of L5 tumor cells expressing no FasL, wtFasL, sFasL, or mFasL for 18 h. Neutrophils stimulated with LPS served as a positive control. Data are presented as mean MIP-2 (A) or IL-1 β (B) concentration in picograms per milliliter \pm SEM. $n = 5$. *, Significant from both L5-neo (Fas⁺) and L5-wtFasL (Fas⁻) at $p < 0.001$; **, significant from both L5-neo (Fas⁺) and L5-mFasL (Fas⁻) at $p < 0.001$; #, significant from both L5-neo (Fas⁺) and L5-mFasL (Fas⁻) at $p < 0.001$.



(22). The level of activated TGF- β in AqH is greatly influenced by 1) the species used, 2) isolation technique, 3) handling, and 4) storage (16, 22, 23). Therefore, studies using fresh AqH to assess the suppressive effects of TGF- β may be quite variable. On the basis of these findings we assessed the ability of 1) fresh and 2) transiently acidified AqH to block IL-1 β production by neutrophils stimulated with the different L5 derivatives. Transient acidification of AqH activates all latent TGF- β .

In the absence of AqH, L5-mFasL tumor cells stimulate neutrophils to produce significant amounts of IL-1 β (60 ± 5.8 pg/ml), whereas L5-wtFasL tumor cells stimulate neutrophils to produce much smaller amounts of IL-1 β (6.0 ± 0.8 pg/ml) (Fig. 6). Neutrophil production of IL-1 β in the presence of fresh AqH was reduced by 47% when stimulated with wtFasL tumor cells and by only 23% when stimulated with mFasL tumor cells. A much more substantial reduction was observed when the same experiment was performed using activated AqH. IL-1 β production by neutrophils was reduced by nearly 90% when stimulated with wtFasL tumor cells, but only by 50% when stimulated with mFasL tumor cells. Taken together, these data demonstrate that the microenvironment of the eye alone is unable to block the proinflammatory effects of tumor cells expressing high levels of mFasL.

High levels of mFasL are required to terminate immune privilege

To ascertain whether the level of mFasL determines the initiation of ocular inflammation and/or the termination of immune privilege, a clone of L5178Y-R tumor cells was established that expressed a lower level of mFasL (L5-mFasL^{low}), as compared with the level of mFasL on tumor cells used in the previous experiments (Fig. 1B). These clones were injected into both the AC and s.c. sites. As a positive control, L5-neo tumor cells (FasL negative) grew progressively in either the s.c. (Fig. 7A), or the AC sites (Fig. 7B). As shown here and in the previous experiments, L5-mFasL tumors expressing high levels of mFasL (L5-mFasL) were rejected from either the s.c. or the AC sites. By contrast, L5-mFasL^{low} tumors were rejected from the s.c. site (Fig. 7A), but not the AC site (Fig. 7B). Histological studies revealed a low level of inflammation present early following injection of L5-mFasL^{low} tumors into the AC site, as demonstrated by a neutrophil infiltrate (data not shown). However, the level of infiltration was insufficient to terminate immune privilege. We conclude from these data that only tumors with high levels of mFasL terminate immune privilege, whereas immune privilege remains intact for tumors that express low levels of mFasL.

In addition, these data also reveal an interesting point. L5 tumors with low levels of mFasL were rejected from the s.c. site, but

these same tumor cells grew progressively within the AC site. This indicates that the level of mFasL required to initiate inflammation that successfully rejects tumors is significantly lower in nonimmune privileged sites, such as the s.c. site, as compared with the privileged AC of the eye.

L5178Y-R lymphoma cells expressing mFasL are not rejected in SCID/beige mice

SCID/beige mice were used to determine whether neutrophils, in the absence of an adaptive immune response, are capable of completely eliminating L5-mFasL tumors from the eye. SCID/beige mice received injections of L5 cells expressing the different forms of FasL. Tumor growth within the AC was assessed by slit lamp microscopy, and the results are displayed as the percentage of the AC containing tumor (Fig. 8A). Survival of tumor-bearing mice (Fig. 8B) was also observed (Fig. 8B). As expected, L5-neo or L5-sFasL tumors grew progressively, and no mice survived past day 20

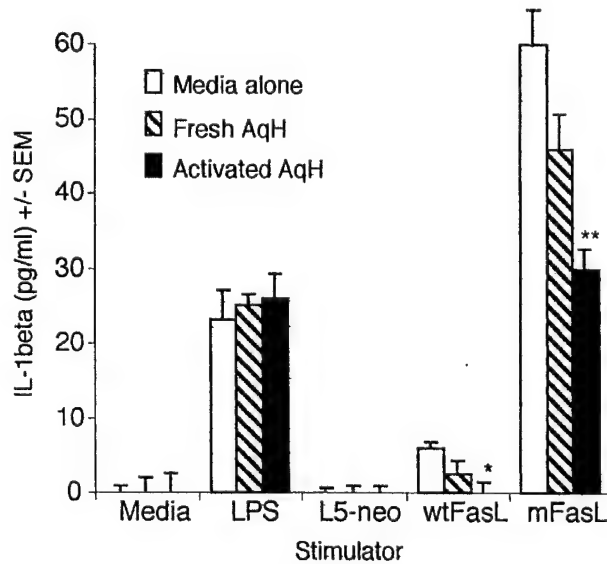
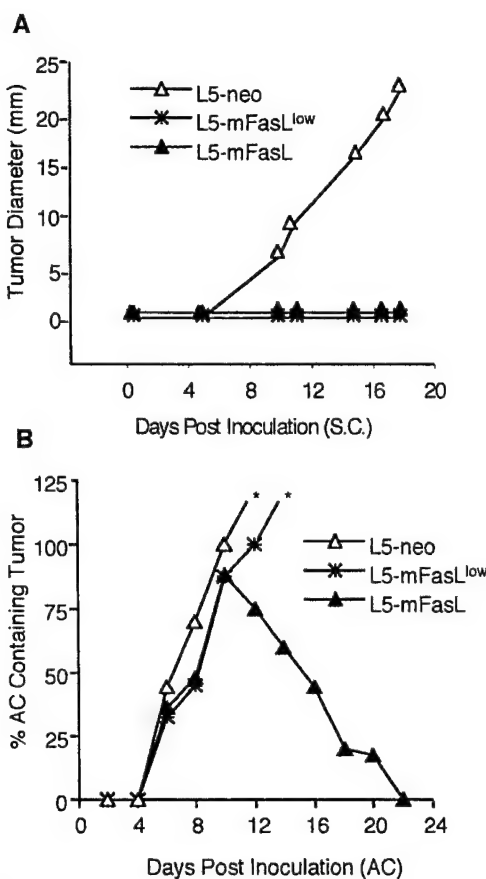


FIGURE 6. AqH inhibits neutrophil production of IL-1 β . Neutrophils (6×10^4 cells/well) were isolated from DBA/2 mice and incubated for 18 h with L5 derivatives (1.2×10^5 cells/well) in serum-free medium containing no AqH, 50% fresh AqH, or 50% activated AqH. Neutrophils stimulated with LPS served as a positive control. Data are presented as mean IL-1 β concentration in picograms per milliliter \pm SEM. $n = 6$. *, Significant from L5-wtFasL cultures containing no AqH at $p < 0.01$; **, significant from L5-mFasL cultures containing no AqH at $p < 0.01$.



postinoculation. Interestingly, although L5-mFasL tumors eventually grew progressively, there was a significant delay in tumor growth during the first 20 days postinoculation. Moreover, although all mice eventually succumbed to L5-mFasL tumors, these mice survived significantly longer (day 30) as compared with the other groups of mice (day 20). We conclude that, in the absence of T cells, NK cells, and B cells, neutrophils are capable of eliminating some tumor cells and slowing the growth of ocular tumors. However, expression of mFasL is unable to bring about complete

elimination of all tumor cells from the immune privileged ocular compartment of SCID/beige mice. These data suggest that an early nonspecific neutrophil-mediated inflammatory response is followed by an adaptive immune response that is ultimately responsible for rejecting the ocular tumor.

SCID/beige mice mount an early neutrophil-mediated immune response against L5-mFasL tumors

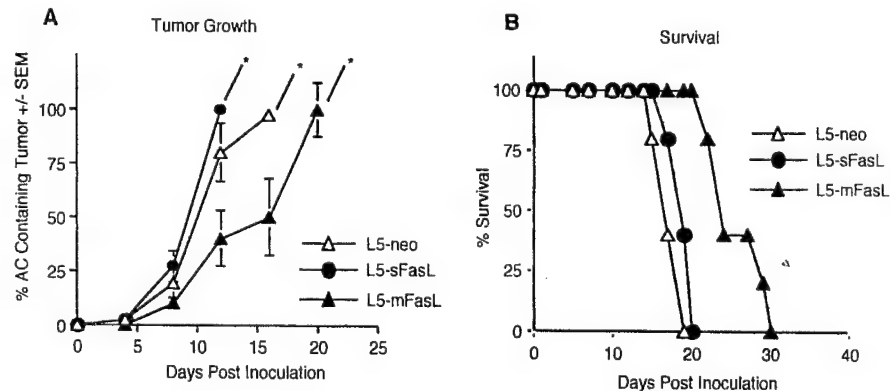
To determine whether the delay in ocular tumor growth in SCID/beige mice coincides with infiltration of neutrophils into the tumor-containing eye, a histological analysis was performed. As a control, tumor growth in SCID/beige mice was compared with tumor growth in DBA/2 mice. Tumor cells expressing no FasL grew to fill the AC with solid tumor, and there was no evidence of any inflammatory infiltrate in either SCID/beige or DBA/2 mice (Fig. 9). By contrast, an intense neutrophil-mediated inflammatory response was present in the cornea and AC of both DBA/2 and SCID/beige mice injected with L5-mFasL cells (Fig. 9). These data indicate that the delay in growth of AC L5-mFasL tumors coincides with extensive neutrophil infiltration. However, in the absence of an adaptive immune response, the neutrophils alone are not sufficient to eliminate ocular tumors completely.

Rejection of ocular L5-mFasL tumors confers systemic tumor-specific immunity

To determine whether rejection of L5-mFasL ocular tumors results in long term systemic protective immunity, DBA/2 mice that had completely eliminated L5-mFasL tumors from the AC were given a secondary tumor challenge in the flank (s.c.) with L5-neo tumor cells. Because these secondary tumors are FasL negative, only mice with systemic protective antitumor immunity would be expected to survive. As a negative control, naive mice (without a previous ocular tumor) received a similar tumor s.c. challenge in the flank. As expected, tumors grew progressively within the flank of naive mice (Fig. 10). By contrast, mice that had previously rejected L5-mFasL tumors from the AC were protected completely and eliminated FasL-negative tumors injected s.c. We conclude that rejection of tumors expressing mFasL from the eye results in acquisition of systemic protective antitumor immunity. In addition, these results imply that the early nonspecific inflammatory response induced during rejection of L5-mFasL tumors results in activation of tumor-specific T cells that are ultimately responsible for protective immunity.

Discussion

Medewar (24) first described the concept of immune privilege in the 1940s, when he observed that skin grafts placed in the anterior



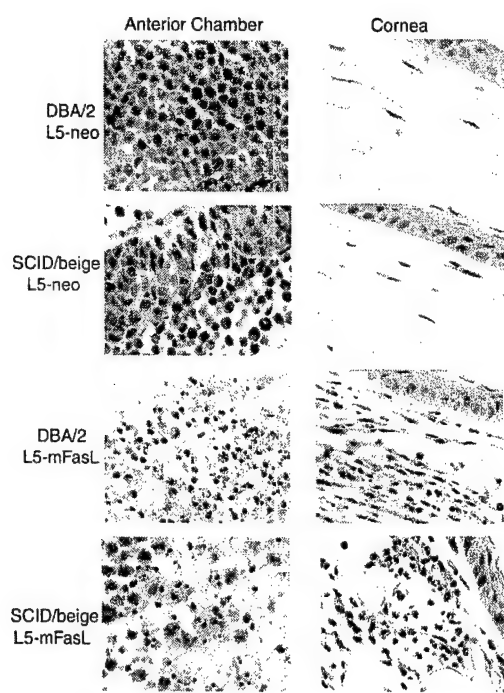


FIGURE 9. L5-mFasL tumor cells trigger a neutrophil-mediated inflammatory response in both DBA/2 and SCID/beige mice. DBA/2 and SCID/beige mice received AC inoculations of 2×10^3 L5-neo or L5-mFasL cells. Histological analysis of the L5 derivatives was performed at 6 days postinoculation. Progressive tumor growth in the AC and clear corneas were observed in both DBA/2 and SCID/beige mice inoculated with L5-neo cells. In contrast, both DBA/2 and SCID/beige mice inoculated with L5-mFasL cells exhibited tumor regression and fibrosis within the AC that was accompanied with massive neutrophil infiltration throughout the cornea. Magnification, $\times 100$.

chamber of the eye survived for prolonged periods of time. Although much progress has been made in the last three decades in understanding how ocular immune privilege is established and maintained, the exact mechanism(s) responsible for this unique phenomenon remains under investigation. Because the anterior

chamber lacks direct lymphatic drainage and possesses a blood-ocular barrier, it was first thought that ocular immune privilege was due solely to the presence of a physical barrier that blocked the egress and infiltration of immune cells (25). This concept has since been challenged, and it is now known that ocular immune privilege is actively maintained. In addition to the blood-ocular barrier, the production of soluble factors, such as TGF- β (22, 26), and the expression of cell surface molecules, such as FasL (3, 27), act together to maintain the immune privileged environment of the eye.

FasL is constitutively expressed in the eye and is thought to protect ocular integrity and maintain immune privilege by inducing apoptosis in infiltrating Fas $^+$ immune cells (3). Previous studies have demonstrated that the constitutive expression of FasL on the cornea plays a significant role in corneal allograft survival (27, 28). Using a murine model of corneal transplant, both Stuart et al. (27) and Yamagami et al. (28) showed that FasL-positive grafts were accepted 45–50% of the time whereas FasL-negative corneal grafts were rejected nearly 100% of the time.

Interestingly, although expression of FasL within the eye appeared to be immunoprotective, transplantation experiments conducted at nonocular sites revealed that FasL could be either immunoprotective (4, 5, 8) or immunodestructive (6, 9). In an effort to resolve these conflicting data, Chen et al. demonstrated that colon carcinoma cells transfected with wtFasL were proinflammatory when injected into a nonprivileged site (s.c. tissue), but the same tumor cells failed to induce an inflammatory response when injected into an immune-privileged site (AC) (9). Their data indicated that TGF- β , which is present in AqH within the anterior chamber, inhibited the ability of FasL-positive tumor cells to activate neutrophils. They concluded that the microenvironment determined the function of FasL; within immune-privileged sites FasL is noninflammatory, and within nonprivileged sites FasL is proinflammatory.

We observed similar results using lymphoma cells that expressed wild-type FasL that were injected into the AC. These tumor cells grew progressively and failed to initiate either ocular inflammation, or neutrophil infiltration. By contrast, injection of L5-mFasL cells that expressed only mFasL into the AC of the eye 1) terminated immune privilege, 2) initiated tumor rejection and vigorous ocular inflammation, 3) induced extensive infiltration of neutrophils into the tumor-containing eye, and 4) activated neutrophils (*in vitro*) to secrete MIP-2 and IL-1 β . These results for mFasL tumor cells were surprising because L5-wtFasL tumors express both mFasL and sFasL and had no effect on ocular immune privilege.

One interpretation of these data is that there is a threshold level of mFasL that is required to initiate inflammation within the immune-privileged eye. Our data demonstrate that only tumor cells expressing high levels of mFasL are able to trigger ocular inflammation and tumor rejection, whereas tumor cells expressing low levels of mFasL (L5-wtFasL and L5-mFasL^{low}) are only able to trigger mild inflammation that fails to terminate privilege, and the tumors grow progressively. Interestingly, both L5-mFasL^{high} and L5-mFasL^{low} tumors triggered potent antitumor inflammation and were completely rejected from the nonimmune privileged s.c. tissue of the flank. Taken together, these data clearly support the idea that 1) high levels of mFasL are required to initiate inflammation and terminate immune privilege within the eye and 2) the threshold level of mFasL required to initiate inflammation is much higher within the immune-privileged eye than within the non-immune-privileged s.c. tissue of the flank.

The fact that low levels of mFasL initiate vigorous inflammation and tumor rejection in nonprivileged sites, whereas significantly

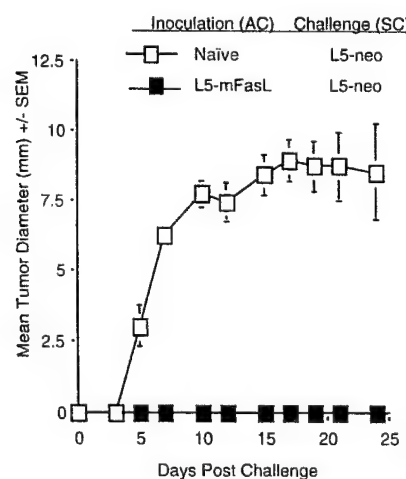


FIGURE 10. Rejection of ocular L5-mFasL tumors confers protection from a secondary s.c. challenge of L5-neo tumor cells. DBA/2 mice received AC inoculations of 2×10^3 L5-mFasL cells, and at 40 days postinoculation these mice received a second tumor challenge of L5-neo cells injected into the s.c. tissue of the flank. Mean tumor diameter was measured every 2 days. Data were pooled from two independent experiments. $n = 10$ (naive) and $n = 8$ (immunized).

higher levels of membrane FasL are required to achieve the same effect within the immune-privileged eye, raises an important question of how the eye down-regulates or blocks the proinflammatory function of mFasL. One likely source of regulation is the unique ocular microenvironment within the AC of the eye, which is filled with AqH that contains soluble immunomodulatory factors (TGF- β , α -melanocyte-stimulating hormone, vasoactive intestinal peptide, calcitonin gene-related peptide) (21, 22, 26, 29–31). These soluble factors may block directly the expansion of the inflammatory cascade initiated by mFasL tumor cells by inhibiting the release of chemokines and proinflammatory cytokines from Fas-positive neutrophils.

Chen et al. (9) concluded from their TGF- β studies that the microenvironment within the eye and not the level of FasL expressed on tumor cells determined whether wtFasL tumor cells induced inflammation. We observed similar results using tumor cells expressing wtFasL, demonstrating that AqH blocked completely the release of IL-1 β from neutrophils stimulated with wt-FasL tumor cells. By contrast, AqH failed to block completely the release of IL-1 β from neutrophils stimulated with tumor cells expressing high levels of mFasL. Taken together, these data demonstrate that the form and level of FasL are critical in determining function, because the suppressive microenvironment within the eye cannot block the proinflammatory effects of tumor cells expressing high levels of mFasL.

Although our studies demonstrate the suppressive nature of AqH, which specific factor(s) blocks the proinflammatory effects of mFasL is under investigation. Chen et al. have shown TGF- β is involved; however, there are many other factors present in the AqH, including soluble FasL. Recent studies demonstrate that sFasL is not only noninflammatory but can also actively inhibit mFasL-induced inflammation (13, 14). Therefore, we predict the environment within the eye uses multiple soluble factors, including sFasL to increase the threshold level of mFasL required to initiate vigorous inflammation. Experiments are in progress to test this prediction.

In addition to elucidating the mechanism(s) by which the eye increases the threshold of mFasL required to induce inflammation, it is important to identify the target cell population FasL initially triggers on injection into the AC. Although our studies clearly demonstrate that neutrophil-mediated inflammation coincides with tumor rejection within the AC of the eye, these studies do not rule out the possibility that the FasL expressed on tumor cells initially triggers a target population other than neutrophils, which release chemotactic factors for neutrophils. Previous studies using a peritoneal tumor model demonstrate that mFasL expressed on tumor cells actually triggers resident macrophages that in turn release chemotactic factors for neutrophils (13, 32). Furthermore, although functional Fas is required on host cells to trigger the neutrophil response, the neutrophils themselves do not require Fas expression (13). Therefore, although our experiment using neutrophils from Fas-deficient MRL-lpr mice demonstrates the importance of functional Fas for both IL-1 β and MIP-2 production, it is possible that the Fas expressed on the 1–2% nonneutrophil cells present in our cell preparation is actually the critical factor. This would require that only a few Fas-expressing cells (nonneutrophils) triggered by mFasL would be sufficient to activate neutrophils.

Because neutrophils are not normally present within the AC of the eye, it is more likely that there is a population of cells other than neutrophils that is the initial target of mFasL tumor cells. When injected into the AC, the tumor cells grow first at the angle of the iris and cornea. Therefore, it is possible that the mFasL triggers the macrophages/dendritic cells present in the iris to release factors such as IL-1 β and MIP-2, which in turn recruit neu-

trophils to the site. Although our studies clearly demonstrate that neutrophil-mediated inflammation coincides with tumor rejection in the AC, the initial target cell population triggered by mFasL remains unclear. Additional studies are under way to identify this population and to assess the importance of Fas expression on cells resident within the eye and on the neutrophils recruited to the eye.

Another intriguing aspect of our data was the observation that activation of neutrophils alone was insufficient to eliminate completely ocular L5 tumors that express high levels of mFasL. The fact that SCID/beige mice (with a full complement of neutrophils) are unable to reject L5-mFasL tumors indicates that an adaptive immune response is necessary for complete tumor eradication. Our results also demonstrate that mice that have rejected ocular L5-mFasL tumors acquire protective systemic antitumor immunity and are capable of eliminating a subsequent tumor challenge in the flank. Expression of protective immunity is independent of FasL, because FasL $^{-}$ tumor cells were used in the second tumor challenge. Although additional experiments are required, these data suggest that tumor-specific T cells mediate protective immunity and that these effector cells ultimately reject the intraocular tumor cells. If this occurs, it would be surprising, because the long-standing dogma regarding the Fas-FasL system and immune privilege has been that the expression of FasL on ocular tissues maintains immune privilege by eliminating infiltrating T lymphocytes and other inflammatory cells.

Therefore the question becomes, "Why are the Fas $^{+}$ T cells not eliminated by the FasL $^{+}$ tumor cells?" Recent studies have demonstrated that the FasL can transduce signals via the Fas receptor using nonapoptotic pathways in monocytes (33), dendritic cells (34), and T cells (35). In addition, studies have shown that CD4 $^{+}$ T cells and CD8 $^{+}$ T cells exhibit different sensitivities to Fas-mediated apoptosis (36, 37). In particular, CD4 $^{+}$ Th1 cells are more sensitive to Fas-mediated apoptosis than are CD4 $^{+}$ Th2 or CD8 $^{+}$ T cells. Therefore, tumor rejection could be mediated through cytotoxic CD8 $^{+}$ T cells and CD4 $^{+}$ Th2 cells.

In conclusion, the current study clearly demonstrates that both the form and level of FasL expressed within the eye is critical in immune privilege. sFasL is unable to promote an inflammatory response, resulting in progressive tumor growth. By contrast, mFasL terminates immune privilege and facilitates both a potent innate and adaptive immune response, which together reject the tumor. Furthermore, there is a threshold level of mFasL required to initiate inflammation that successfully rejects tumors in the immune-privileged eye, and this threshold is higher in privileged than in nonprivileged sites.

Acknowledgments

We thank Drs. Andrew W. Taylor and Peter W. Chen for their invaluable help with the AqH experiments. We also thank Jian Gu for technical assistance with histology and Drs. Robert L. Hendricks and J. Wayne Strelein for critical review of the manuscript.

References

- Nagata, S., and P. Goldstein. 1995. The Fas death factor. *Science* 267:1449.
- Nagata, S., and T. Suda. 1995. Fas and Fas ligand: *lpr* and *gld* mutations. *Immunol. Today* 16:39.
- Griffith, T., T. Brunner, S. M. Fletcher, D. R. Green, and T. A. Ferguson. 1995. Fas Ligand-induced apoptosis as a mechanism of immune privilege. *Science* 270:1189.
- Bellgrau, D., D. Gold, H. Selawry, J. Moore, A. Franzusoff, and R. C. Duke. 1995. A role for CD95 ligand in preventing graft rejection. *Nature* 377:630.
- Lau, H. T., M. Yu, A. Fontana, and C. J. Stoeckert. 1995. Prevention of islet allograft rejection with engineered myoblasts expressing FasL in mice. *Science* 273:109.
- Kang, S. M., D. B. Schneider, Z. Lin, D. Hanahan, D. A. Dickey, P. G. Stock, and S. Backeskov. 1997. Fas ligand expression in islets of Langerhans does not confer immune privilege and instead targets them for rapid destruction. *Nat. Med.* 7:738.

7. Turvey, S. E., V. Gonzalez-Nicolini, C. I. Kingsley, A. T. Larregina, P. J. Morris, M. G. Castro, P. R. Lowenstein, and K. J. Wood. 2000. Fas ligand-transfected myoblasts and islet cell transplantation. *Transplantation* 69:1972.
8. Porter, C. J., J. E. Ronan, and M. J. D. Cassidy. 2000. Fas-Fas-ligand antigen expression and its relationship to increased apoptosis in acute renal transplant rejection. *Transplantation* 69:1091.
9. Chen, J.-J., Y. Sun, and G. J. Nabel. 1998. Regulation of the proinflammatory effects of Fas ligand (CD95L). *Science* 282:1714.
10. Kayagaki, N., A. Kawasaki, T. Ebata, H. Ohmoto, S. Ikeda, S. Inoue, K. Yoshino, K. Okumura, and H. Yagita. 1995. Metalloproteinase-mediated release of human Fas ligand. *J. Exp. Med.* 182:1777.
11. Mariani, S. M., B. Matiba, C. Baumler, and P. H. Krammer. 1995. Regulation of cell surface APO-1/Fas (CD95) ligand expression by metalloproteinases. *Eur. J. Immunol.* 25: 2303.
12. Tanaka, M., T. Itai, M. Adachi, and S. Nagata. 1998. Downregulation of Fas ligand by shedding. *Nat. Med.* 4:31.
13. Hohlbaum, A. M., S. Moe, and A. Marshak-Rothstein. 2000. Opposing effects of transmembrane and soluble Fas ligand expression on inflammation and tumor cell survival. *J. Exp. Med.* 191:1209.
14. Suda, T., H. Hashimoto, M. Tanaka, T. Ochi, and S. Nagata. 1997. Membrane Fas ligand kills human peripheral blood T lymphocytes, and soluble Fas ligand blocks the killing. *J. Exp. Med.* 186:2045.
15. Taylor, A. W., P. Alard, D. G. Yee, and J. W. Streilein. 1997. Aqueous humor induces transforming growth factor- β (TGF- β)-producing regulatory T-cells. *Curr. Eye Res.* 16:900.
16. Lawrence, D. A. 1991. Identification and activation of latent transforming growth factor β . *Methods Enzymol.* 198:327.
17. Streilein, J. W., J. Y. Niederkorn. 1981. Induction of anterior chamber associated immune deviation requires an intact, functional spleen. *J. Exp. Med.* 153:1058.
18. Luckenbach, M. W., J. W. Streilein, and J. Y. Niederkorn. 1985. Histopathologic analysis of intraocular allogeneic tumors in mice. *Invest. Ophthalmol. Vis. Sci.* 26:1368.
19. Kernacki, K. A., R. P. Barrett, J. A. Hobden, and L. D. Hazlett. 2000. Macrophage inflammatory protein-2 is a mediator of polymorphonuclear neutrophil influx in ocular bacterial infection. *J. Immunol.* 164:6576.
20. Rudner, X. L., K. A. Kernacki, R. P. Barrett, and L. D. Hazlett. 2000. Prolonged elevation of IL-1 in *Pseudomonas aeruginosa* ocular infection regulates macrophage-inflammatory protein-2 production, polymorphonuclear neutrophil persistence, and corneal perforation. *J. Immunol.* 164:6576.
21. Streilein, J. W., G. A. Willbanks, A. W. Taylor, and S. Cousins. 1992. Eye-derived cytokines and the immunosuppressive intraocular microenvironment: a review. *Curr. Eye Res.* 11(Suppl.):41.
22. Cousins, S. W., M. M. McCabe, D. Danielpour, and J. W. Streilein. 1991. Identification of transforming growth factor- β as an immunosuppressive factor in aqueous humor. *Invest. Ophthalmol. Vis. Sci.* 32:2201.
23. Lyons, R. M., J. Keski-Oja, and H. L. Moses. 1988. Proteolytic activation of latent transforming growth factor- β from fibroblast-conditioned medium. *J. Cell Biol.* 106:1659.
24. Medewar, P. B. 1945. A second study of the behavior and fate of skin homografts in rabbits. *J. Anat. Lond.* 79:157.
25. Medewar, P. B. 1948. Immunity to homologous grafted skin. III. The fate of skin homografts transplanted to the brain, to subcutaneous skin, and to the anterior chamber of the eye. *Br. J. Exp. Pathol.* 29:58.
26. Granstein, R., R. Staszewski, T. L. Knisely, E. Zeira, R. Nazareno, M. Latina, and D. M. Albert. 1990. Aqueous humor contains transforming growth factor- β and a small ($J. Immunol.$ 144:3021).
27. Stuart, P. M., T. S. Griffith, N. Usui, J. Pepose, X. Yu, and T. A. Ferguson. 1997. CD95 ligand (FasL)-induced apoptosis is necessary for corneal allograft survival. *J. Clin. Invest.* 99:396.
28. Yamagami, S., H. Kawashima, and T. Tsuru. 1997. Role of Fas-Fas ligand interactions in the immunorejection of allogeneic mouse corneal transplants. *Transplantation* 64:1107.
29. Taylor, A. W., J. W. Streilein, and S. W. Cousins. 1992. Identification of alpha-melanocyte stimulating hormone as a potential immunosuppressive factor in aqueous humor. *Curr. Eye Res.* 11:1199.
30. Taylor, A. W., J. W. Streilein, and S. W. Cousins. 1994. Immunoreactive vasoactive intestinal peptide contributes to the immunosuppressive activity of normal aqueous humor. *J. Immunol.* 153:1080.
31. Taylor, A. W., D. G. Yee, and J. W. Streilein. 1998. Suppression of nitric oxide generated by inflammatory macrophages by calcitonin gene-related peptide in aqueous humor. *Invest. Ophthalmol. Vis. Sci.* 39:1372.
32. Hohlbaum, A. M., M. S. Gregory, S.-T. Ju, and A. Marshak-Rothstein. 2001. Fas ligand engagement of resident peritoneal macrophages in vivo induces apoptosis and the production of neutrophil chemotactic factors. *J. Immunol.* 167:6217.
33. Daigle, I., B. Ruckert, G. Schnetzler, and H. Simon. 2000. Induction of the IL-10 gene via the Fas receptor in monocytes: an anti-inflammatory mechanism in the absence of apoptosis. *Eur. J. Immunol.* 30:2991.
34. Rescigno, M., V. Piguet, B. Valzasina, S. Lens, R. Zubler, L. French, V. Kindler, J. Tschopp, and P. Ricciardi-Casagnoli. 2000. Fas engagement induces the maturation of dendritic cells (DCs), the release of interleukin (IL)-1 β , and the production of interferon α in the absence of IL-12 during DC-T cell cognate interaction: a new role for Fas ligand in inflammatory responses. *J. Exp. Med.* 192:1661.
35. Suzuki, I., and P. J. Fink. 1998. Maximal proliferation of cytotoxic T lymphocytes requires reverse signaling through Fas ligand. *J. Exp. Med.* 187:123.
36. Zheng, L., G. Fisher, R. E. Miller, J. Peschon, D. H. Lynch, and M. J. Lenardo. 1995. Induction of apoptosis in mature T cells by tumor necrosis factor. *Nature* 377:348.
37. Ehl, S., U. Hoffman-Rohrer, S. Nagata, H. Hengartner, and R. Zinkernagel. 1996. Different susceptibility of cytotoxic T cells to CD95(Fas/APO-1) ligand-mediated cell death after activation in vitro versus in vivo. *J. Immunol.* 156:2357.

Project 3. Restoration of Endothelial Function of the Damaged Cornea
Investigator: **Dr. Nancy Joyce**

Body:

There were a number of accomplishments which emanated from this research. We tested a variety of temperature-sensitive polymers (PIPAAm polymers) for their ability to support growth and non-enzymatic release of corneal endothelial cells as “sheets” from culture dishes. We initiated a collaboration with Dr. Jeffrey Ruberti, Cambridge Polymer Group, Somerville, MA, to develop another method of preparing human corneal endothelial cell “sheets” for transplantation. In addition, we tested the effect of specific growth-promoting agents on proliferation of human corneal endothelial cells to obtain optimal culture conditions and initiated development of an artificial cornea by testing the ability of human corneal endothelial cells to attach and form a normal monolayer on a human corneal fibroblast-derived stromal matrix.

Key Research Accomplishments:

- Tested temperature-sensitive polymers for use in corneal endothelial transplantation
- Tested growth promoting agents to obtain optimal conditions for use in corneal endothelial transplantation
- Initiated development of artificial cornea

Reportable Outcomes:

Zhu CC, Joyce NC. Induction of proliferation in cultured human corneal endothelial cells (HCEC). 2002 annual meeting of the Association for Research in Vision and Ophthalmology (ARVO).

Zieske J, Hutcheon A, Guo X, Joyce N. Human corneal organotypic cultures using untransformed cells. 2002 Gordon Conference on “Signal Transduction by Engineered Extracellular Matrices”.

Conclusions:

The temperature-sensitive polymers tested support growth of corneal endothelial cells. They promote non-enzymatic release of subconfluent cells from the culture dish after lowering the temperature from 37°C to 22°C, but fully confluent monolayers do not readily release as intact cell “sheets”. This result indicates that these polymers are not appropriate to support release of corneal endothelial cells as “sheets” for subsequent transplantation.

We plan to initiate tests using native collagen matrices and positive/negative pressure to promote growth of human corneal endothelial cells and release of the intact monolayer as a “sheet”.

A combination of FBS, EGF, NGF, and pituitary extract (containing high levels of FGF) promotes proliferation of corneal endothelial cells from older donors (> 50 years old) to a level similar to that of FBS alone. The benefit of combining these factors is that, together, they promote the formation of a more compact layer of cells with a morphology similar to that of cells from younger donors.

Human corneal endothelial cells seeded onto a construct consisting of corneal keratocytes and their native matrix will attach, grow, and form a monolayer with excellent morphology. This construct will form the basis for the development of an artificial cornea.

References:

- Chen K-H, Azar D, Joyce NC. Transplantation of adult human corneal endothelium. *Cornea*. 2001;20:731-737.
- Yamato M, Konno C, Utsumi M, Kikuchi A, Okano T. Thermally responsive polymer-grafted surfaces facilitate patterned cell seeding and co-culture. *Biomaterials*. 2002;23:561-7.
- Yamato M, Utsumi M, Kushida A, Konno C, Kikuchi A, Okano T. Thermo-responsive culture dishes allow the intact harvest of multilayered keratinocyte sheets without dispase by reducing temperature. *Tissue Eng*. 2001;7:473-80.
- Kushida A, Yamato M, Konno C, Kikuchi A, Sakurai Y, Okano T. Temperature-responsive culture dishes allow nonenzymatic harvest of differentiated Madin-Darby canine kidney (MDCK) cell sheets. *J. Biomed. Mater. Res.* 2000;51:216-223.
- Kushida A, Yamato M, Konno C, Kikuchi A, Sakurai Y, Okano T. Decrease in culture temperature releases monolayer endothelial cell sheets together with deposited fibronectin matrix from temperature-responsive culture surfaces. *J. Biomed. Mater. Res.* 1999;45:355-362.
- Zieske JD, Mason VS, Wasson ME, Meunier SF, Nolte CJ, Fukai N, Olsen BR, Parenteau NL. Basement membrane assembly and differentiation of cultured corneal cells: importance of culture environment and endothelial cell interaction. *Exp. Cell Res.* 1994;214:621-33.

Appendices:

None.

Project 4. Remote Diagnosis of Retinal Damage

Investigator: **Dr. Ann Elsner**

Body:

The goal of this project is to develop a portable prototype instrument that can image the retina to determine if there has been damage, e.g. laser injury or trauma, that will influence central vision.

One-year goal--- to produce portable prototype of an instrument that can determine if retina has sustained damage that will impact central vision.

Budget includes Dr Ann Elsner (100%) one electronic specialist, one data entry assistant, computer hardware and peripheral and electronics supplies.

A protocol for the testing of human subjects with the portable scanner, and corresponding informed consent form, were prepared and submitted for review. Following the grant proposal, the human subjects submission and the technical and patent work were all performed in parallel. This is a good strategy since the device had clear-cut specifications and safety standards, but takes many months of technical work prior to be ready for testing on a human.

The proposal for Years 1 and 2 was broken up into Tasks 1, 2, 3, and 4. Task 1 uses only a model eye and no human subjects. The power requirements and basic assessment of image quality are readily performed using a model eye and standard laboratory test equipment. Task 2 is the testing of laboratory normal volunteers. Task 3 is the testing of patients who have already been diagnosed with retinal trauma. Task 4 is the testing of actual acute retinal trauma patients. Items have been submitted to seek approval for Tasks 1 – 3, and Task 1 is approved and underway. At this time, Tasks 2-3 are under review. The sequence was as follows:

Initial submission of the protocol for testing of the device with human subjects and the corresponding consent form to the Institutional Review Board of the Schepens Eye Research Institute in the usual format, followed by approval of these items.

Re-submission to the Institutional Review Board of the Schepens Eye Research Institute, including revision to the Department of Defense style format. As this review board had considered virtually only National Institute of Health or private foundation style grants throughout the tenure of the current and past chairs and most committee members, Dr. Elsner included the specific instructions from Louise M. Pascal,RN,MS, Human Subjects Protection Specialist (AMDEX Corporation). These instructions concerned the points to be covered in a review for the U.S. Army Medical Research and Materiel Command, Office of Regulatory Compliance and Quality and the corresponding regulations, which Dr. Elsner and staff downloaded from the many, pertinent websites. The resulting document was over 200 pages and described the differences in several sections, including the format of both the protocol and consent form, the specific wording for reporting, the signature block, and other items. The safety in terms of not greater than minimal risk was considered and approved by the committee, and the appointment of a medical monitor if the device exceeded this was not deemed necessary, although the name and CV of an appropriate physician was included in case this appointment was deemed necessary.

Pre-Submission to Louise Pascal, to evaluate the details of the protocol and consent form prior to review by Office of Regulatory Compliance and Quality, concerning Proposal No. 00171007, HSRRB Log No. A-10379.3. Discussion during a visit by Ms. Pascal and through telephone conversations and Email led to the next submission. Ms. Pascal suggested several changes in format, wording, and location of items, as well as provided information on the changed signature block format and additional forms concerning potential FDA classification and other matters. Another point was to put into the proposal two separate assessments of risk, one for the device and a second for the protocol. The consent forms for Tasks 2 and 3 were made into separate documents. She advised Dr. Elsner to return these materials directly to her office for review, and then to go back to the Institutional Review Board of the Schepens Eye Research Institute with a living document.

Revision of the protocol and re-submission to the Office of Regulatory Compliance and Quality via Louise Pascal. Each item noted by Ms. Pascal was revised or explained. There was a great deal of website work with the newer regulations and FDA materials. It was determined that the classification scheme provided by the FDA was aimed more at devices available outside a single laboratory, but this device could best be classified as "Investigational."

Provisional patent filings

The current policy of the Schepens Eye Research Institute is to file a provisional patent application and to search for sponsorship to support the patent procedure. A provisional patent has been filed by. Holliday C. Heine, Ph.D. of Weingarten, Schurigin, Gagnebin & Hayes LLP. This initial document was based on the work available in September – October, 2001. Additional work led to an updated version with a drawing of the best embodiment in January, 2002.

Discussions with FDA

The FDA has the responsibility to review devices used to image the human retina, such as this one, but actually reviews those intended for commercial development once such a device is to the development stage sufficient to permit review. They do not have the mandate or manpower to evaluate the safety of devices that are still in the early stages of development or those in laboratories. There are clear-cut guidelines for ophthalmic devices, particularly for those scanning devices that image the retina. The chief safety element is that the incident power on the retina be controlled by either maintaining low power for extended viewing, a primary position that deflects the laser beam away from the eye, or an interlock system.

Provisional patent filings

The current policy of the Schepens Eye Research Institute is to file a provisional patent application and to search for sponsorship to support the patent procedure. A provisional patent has been filed by. Holliday C. Heine, Ph.D. of Weingarten, Schurigin, Gagnebin & Hayes LLP. This initial document was based on the work available in September – October, 2001. Additional work led to an updated version with a drawing of the best embodiment in January, 2002.

Technical Development

System Approach - Our goal for the first year is to investigate simplifying the existing scanning laser technology to produce a working prototype that specifically images the central 20 degrees of the retina, readily carried and operated by one person. We have now have proof of principal for the main optical plan. Other than one of our scanning assemblies, we used modestly priced and off-the-shelf components. Further refinements to improve the optics or reduce the size will be undertaken. We have now produced a system that can accomplish this first part. An appropriate size image of good quality is produced (Appendix). The most important aspect is that we have eliminated the unwanted reflections from the anterior segment of the model eye. The major components are small enough to be carried once we provide packaging for our breadboard system. Most of the components now have the capability of being battery operated, with a plan to develop battery operation for the rest. As planned, we are undertaking experiments and are re-designing to reduce the size, which will be followed by further electronics development to make all components run on battery, thereby avoiding

cords and heavy power supplies.

Several of the main features have been investigated by studying consumer digital cameras, ophthalmic instruments, and a wide variety of high-end retinal imaging devices. The controls and storage methods for these devices have been considered. The potential for ease of image transfer and usability is of particular note, and our long term goal is to eliminate the onsite computer and acquisition system, although for development purposes this is very helpful. We reduced weight and moving parts by devising a slit scan technique similar to that used in confocal microscopy. This has one dimension of scanning, in order to paint a moving illuminated slit over the retina, thereby improving contrast over the flood illumination found in a fundus camera. Currently, the input and output pupils are separated, requiring about 2 deg total. The image is approximately 20 degrees visual angle. Once we have permission to test subjects, we plan to determine whether the simplified technology is sufficient to decrease unwanted scatter so that retinal and deeper structures are successfully imaged.

Optics - The choice of an illumination source using near infrared light provides several choices for low power operation. As laser sources, we are currently investigating an 830 nm laser diode with battery operation and Vertical Cavity Surface Emitting Laser (VCSEL elements). We currently are using a 543 nm HeNe laser as well as a near infrared laser, since initial alignment with near infrared is far more difficult: the infrared beam cannot be seen without electronic instrumentation and phosphor cards.

We have had several types of designs, 6 sets to date. The main ones include laser scanning and a two dimensional detector.

Electronics - The raster is painted on the retina with a single moving part that sweeps a slit across the retina, rather than scanning in two dimensions; this is termed slit scanning. Currently, a monochromatic video camera is used, along with a traditional image acquisition board in a computer. This is extremely useful during optical development, since video rate capture permits the detection of stray light and other problems. Our next step towards portability is to use a laptop with a smaller acquisition card in a PCMCIA slot . Future plans are to integrate a CCD or CMOS chip and illumination and scanning onset circuitry, without a computer during image acquisition. This differs from previous instruments to image the retina, most of which use two moving parts to sweep a single laser spot into a two dimensional raster across the retina, used in combination with a single point detector. Currently, we are using a two dimensional detector rather than a linear array.

Design 4 Results - Designs 1 – 4 included only one moving part to generate scanning and a confocal aperture to reduce stray light. For the moving part, we used a resonant galvonometer, without descanning the light returning from the retinal, but included apertures. This plan does not permit a true confocal aperture, which would reduce out of plane scattering sources to a greater extent than merely trimming the light. This scanning hardware was battery operated. An image was produced, and the major reflections minimized by the use of polarizers (Appendix). Until a human eye can be used as a target, development on this plan must wait.

Design 5 Results - Design 5 is unlike any previous design. For the first time we are descanning and then rescanning the light reflected from our model eye. We would like the final product to closely resemble this design configuration. We removed unwanted reflections in this design,

achieving one of our goals which was that no polarizers were used to rid the image of parasitic reflections. An image is shown in the Appendix.

A four-sided custom polygon, a custom order from Electro-Optical Products Corporation, was mounted on top of a Servo-Systems 12 V DC geared motor head. The motor featured variable rotational frequencies from 0 Hz to 12 Hz (4 mirror facets = factor of 4 increase in scanning frequency). We found that this inexpensive, off-the-shelf motor has a little bit of wobble in the vertical direction of the image plane, approximately 0.2 degrees visual angle in the eye (~10 image pixels x 8 um/pixel x 1deg/300um). The polygon facets are also not perfectly orthogonal, which could also be responsible for some of the image wobble. This amount of wobble is acceptable in the proof of principal for the optical concept. Also, as we plan single (still) images, and not video, this is only a problem while we are using the video camera.

We are considering methods to improve image quality and image size with respect to the retina. We determined that the incident slit light on the polygon must be directed very close to its axis to prevent light from slipping by the polygon and entering the imaging elements on the opposite side of the system. This restricts the amount of light reflected from the model eye that can be captured by the descanning imaging optics. It would be ideal to scan the slit light off of the edge of the polygon, in order to maximize the orthogonal polygon face area that captures light reflected from the eye. We noticed some severe aperturing affects in our final model eye "retinal" images and will attempt to track them down in the next design revision.

A second factor that may have a part in restricting the retinal field of view is the distance the model eye and two lenses past the polygon are off axis. This is known as the split pupil design. In Design 5, the input light travels down the right hand side (when facing the model eye) or "channel" of the first lens element, about 8 mm from the 25 mm lens side (1/3 of the lens diameter). This could be too far off axis (or too little), possibly causing these aperturing affects. This will also be explored in more detail in the next revision.

The pupil plane light that enters the model eye may also have positional variation that needs further study. It appears the light is converging at the plane of the lens element of the model eye and not the pupil of the model eye. This may also be one of the causes for the vignetting observed.

Lastly, the confocal aperture optics may also be responsible for the restricted field of view that is observed. A single lens is used to focus light returning from the model eye to a retinal plane (where a confocal aperture will be located) and then used again to transmit that retinal plane light to the polygon for CCD rescanning. Two first surface mirror edges are used to redirect the light through a confocal aperture. The confocal aperture was not used in this design b/c the primary design goal was to demonstrate polygon scanning, descanning and rescanning principals. It could be that some of the descanned light is missing the redirecting mirrors. This will also be examined in greater detail in the design revision.

A second difficulty with the current confocal aperture optical design is that using a single lens element crosses the two paths incident and exiting the confocal aperture. This will make it difficult to physically locate a confocal aperture between the redirecting mirrors.

Results from Design 6 - We reconfigured a portion of the optical pathway to implement changes for Design 6, and made several experiments. The results are given in the Appendix. The illumination path of Design 6 is the same as it was in Design 5, although the light entering the model eye is less off axis in Design 6t. However, several changes were made to the descanned light path for Design 6. The light no longer passes through a single lens element to and from the confocal aperture plane. Instead, it now reflects around a rectangular shaped path through two separate lens elements, which create and re-image the confocal aperture plane. Please see the schematic layout diagram for more details (Appendix).

Our primary goal in Design 6 was to solve the aperturing/vignetting problem we observed in Design 5 results. We suspected this was due to the turning mirrors in the Design 5 descanned light path having such close proximity to the confocal aperture plane (a retinal plane). By separating the descanned light path and using two lens elements, we were able increase our retinal field of view from 10 degrees to about 20 degrees visual angle.

The improved field of view and image quality could also be due to the split pupil distance not being as large as it was in Design 5. In the pupil plane of the model eye, the entering and exiting light paths are now only separated by about 1 mm. It was much larger in Design 5. The affects of the off-axis displacement of split pupil design will be examined in more detail in further designs.

The resulting images for Design 6 displayed the experiments in the use of a confocal aperture. When a confocal aperture was used (a 100 um slit), the light was heavily attenuated, as expected. Certain optical configurations led to no recognizable image, while others gave an image of high contrast of the target in the model eye.

Design 7 will improve the use of the confocal aperture for the enhancement of image contrast, but the exact optical configuration needs to be optimized for a human eye rather than a model eye. We plan to:

Reconfigure confocal pathway

Try various confocal apertures

Determine source of wobble and explore a variety of scanning mechanisms

Explore split pupil/off –axis affects on image quality

Image with the IR diode laser

Assemble IR VCSEL for operation

Expand the beam more, for complete CCD illumination

Software Development - We have begun software development to quantify image features described in the proposal and outcome measures in the human subjects protocol to:

Create function to calculate the contrast ratio in a Region of Interest (ROI).

Calculate Michelson Contrast Ratio for any area of interest, between two features.

Create function to calculate the variation of gray scale level in areas w/o vessels.

Calculate mean, std. deviation, coefficient of variation (CV).

Create function to calculate retinal vessel diameter.

Create a function to calculate the area in number of pixels covered by a certain feature, such as trauma.

Key Research Accomplishments:

- Human Subjects Materials
- Provisional Patent Filings
- Technical Development

Reportable Outcomes:

Elsner, A.E. Remote Diagnosis of Retinal Damage: Subproject 4, "To develop a prototype instrument to image the retina, TATRC Principal Investigators Meeting presentation in association with Medicine Meets Virtual Reality, Newport Beach, CA, January 22, 2002.

Elsner A.E., Stewart J.S. Towards a portable digital retinal imager, to be presented at the Annual meeting of the Optical Society of America, September 30, 2002.

Elsner A.E. device for Digital Retinal Imaging, Provisional Patent Application, initial application and extension with updated drawing.

Conclusions:

We designed a portable retinal scanner device that can eventually be battery operated and portable. We filed a provisional patent on this design, and have made two different realizations that allowed image capture in the laboratory of a model retina. With the later designs, these images were of approximately the correct size with respect to the retina, were free of major unwanted reflection or stray light, and used an amount of light typically approved by the FDA for ophthalmic instruments. We have applied for permission to test human subjects, which will allow the further testing and improvement of this design prior to additional miniaturization. We have begun software development to quantify sample features in these images.

References:

None.

Appendices:

Elsner A.E., Stewart J.S. paper to be presented at the Annual Meeting of the Optical Society of America, September, 2002.

Elsner, A.E. Remote Diagnosis of Retinal Damage: Subproject 4, "To develop a prototype instrument to image the retina," TATRC Principal Investigators Meeting presentation in association with Medicine Meets Virtual Reality, Newport Beach, CA, January 22, 2002.
Optical Schematic from provisional patent and sample CAD drawings.

Image from design 4

Image from design 5

Image from design 6

Towards a portable digital retinal imager

Ann E. Elsner, Ph. D. and Jason B. Stewart
Schepens Eye Research Institute

To be presented at OSA Annual Meeting, September 2002.

A portable, hand-held scanner is being developed to provide high image contrast, yet operate in a manner similar to an everyday digital camera. Additional goals include battery operation and non-invasive, non-mydriatic image acquisition for remote diagnosis of retinal trauma and disease.

Tentative Agenda
Telemedicine and Advanced Technology Research Center (TATRC)
Advanced Medical Technology Principal Investigators Review

***Theme: "Transitioning from the Information Age
Into the Bio-Intelligence Age"***

January 23, 2002

<u>Time</u>	<u>Topic</u>	<u>Presenter</u>
0730 – 0800	<i>Continental Breakfast</i>	
0800 – 0815	Welcome and Introductions	Mr. Conrad Clyburn Telemedicine and Advanced Technology Research Center, USAMRMC
0815 – 0830	The TATRC Perspective	COL Dean Calcagni Telemedicine and Advanced Technology Research Center, USAMRMC
0830 – 0845	Setting the Tone	Dr. Richard Satava Yale University School of Medicine
0845 – 1215	<u>Core Focus Area: Biology</u>	
0845 – 0900	Organ Replacement	Dr. Joseph Vacanti Center for Integration of Medicine and Innovative Technology
0900 – 0915	Remote Diagnosis of Retinal Damage	Dr. Ann Elsner Schepens Eye Research Institute
0915 – 0930	Molecular Regulation of Apoptosis in Wound Healing	Dr. Yong-Jian Geng University of Texas Health Science Center at Houston Medical School
0930 – 0945	Functions of Nitric Oxide and Nitrotyrosine in Shock, Sepsis and Inflammation	Dr. Ward Casscells University of Texas Health Science Center at Houston Medical School
0945 – 1000	MEMS Based Emulations	Dr. Christopher Dubé Draper Laboratories
1000 – 1015	Questions & Answers	
1015 – 1030	<i>Mid-morning Break</i>	
1030 – 1045	Regeneration of the Damaged Central Nervous System	Dr. Dong Feng Chen Schepens Eye Research Institute

TATRC's Advanced Medical Technology Principal Investigators Review
January 23, 2002

<u>Time</u>	<u>Topic</u>	<u>Presenter</u>
1045 – 1100	UP Regulation of P450-A Natural Broad Based Defense Against Chemical and Biological Threats	Dr. Henry Strobel University of Texas Health Science Center at Houston Medical School
1100 – 1115	Müllerian Inhibiting Substance for Treatment of Ovarian Cancer	Dr. David MacLaughlin Center for Integration of Medicine and Innovative Technology
1115 – 1130	Bio and Chemical Warfare Defense	Dr. James Wild Texas A&M University
1130 – 1145	New Advanced Technology to Improve Prediction and Prevention of Type I Diabetes	Dr. Massimo Trucco Children's Hospital of Pittsburgh
1145 – 1200	Cardiomyocyte Repopulation Using Percutaneous Delivery of Tissue Engineered Systems	Dr. Craig Thompson Center for Integration of Medicine and Innovative Technology
1200 – 1215	Questions & Answers	
1215 – 1345	* <i>Lunch</i> Guest Speakers: 1. TBA 2. TBA	
1345 – 1500	<u>Core Focus Area:</u> <u>Computer/Information</u>	
1345 – 1400	High Precision Information Retrieval	Dr. Lawrence Fagan Stanford Medical Informatics
1400 – 1415	Patient-Centric Network	Dr. Nat Sims Center for Integration of Medicine and Innovative Technology
1415 – 1430	Next Generation Internet (NGI)	Dr. Greg Mogel University of Southern California
1430 – 1445	Computer Simulation	Dr. Steve Dawson Center for Integration of Medicine and Innovative Technology
1445 – 1500	Questions & Answers	
1500 – 1515	<i>Mid Afternoon Break</i>	

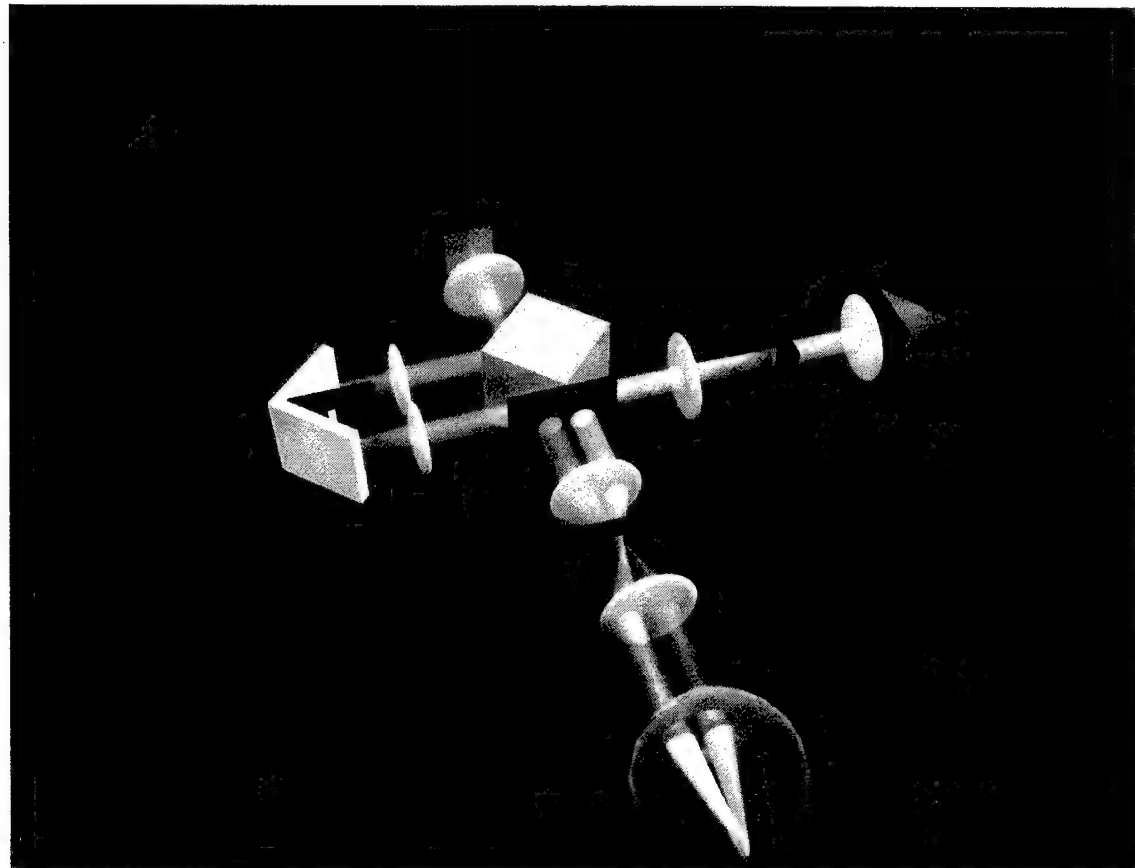
TATRC's Advanced Medical Technology Principal Investigators Review
January 23, 2002

<u>Time</u>	<u>Topic</u>	<u>Presenter</u>
1515 – 1645	<u>Core Focus Area: Engineering</u>	
1515 – 1530	Remote Acoustic Hemostasis	Dr. Larry Crum Applied Physics Lab University of Washington
1530 – 1545	Evaluation of New Axial Flow Pump	Dr. Branislav Radovancevic Texas Heart Institute, Texas Medical Center
1545 – 1600	Real-time 3D Ultrasound	Dr. Raj Shekhar Cleveland Clinic
1600 – 1615	Upgrade of Loma Linda University Proto Synchrotron and Switchyard for performing Beam Scanning of Large Irregular Targets in Human Patients with Cancer	Dr. David Bush Loma Linda University
1615 – 1630	Radio Frequency Triage (RAFT) Tool, a Diagnostic Tool for Combat Medics	Dr. Geoffrey Ling Uniformed Services University of the Health Sciences
1630 – 1645	Periscopic Spine Surgery	Dr. Kevin Cleary Georgetown University Medical Center
1645 – 1700	Summary and Final Closing Statements	Dr. Richard Satava Dr. Gerry Moses Telemedicine and Advanced Technology Research Center, USAMRMC
1700 –	<i>* Evening Reception and Networking Social at Newport Marriott</i>	

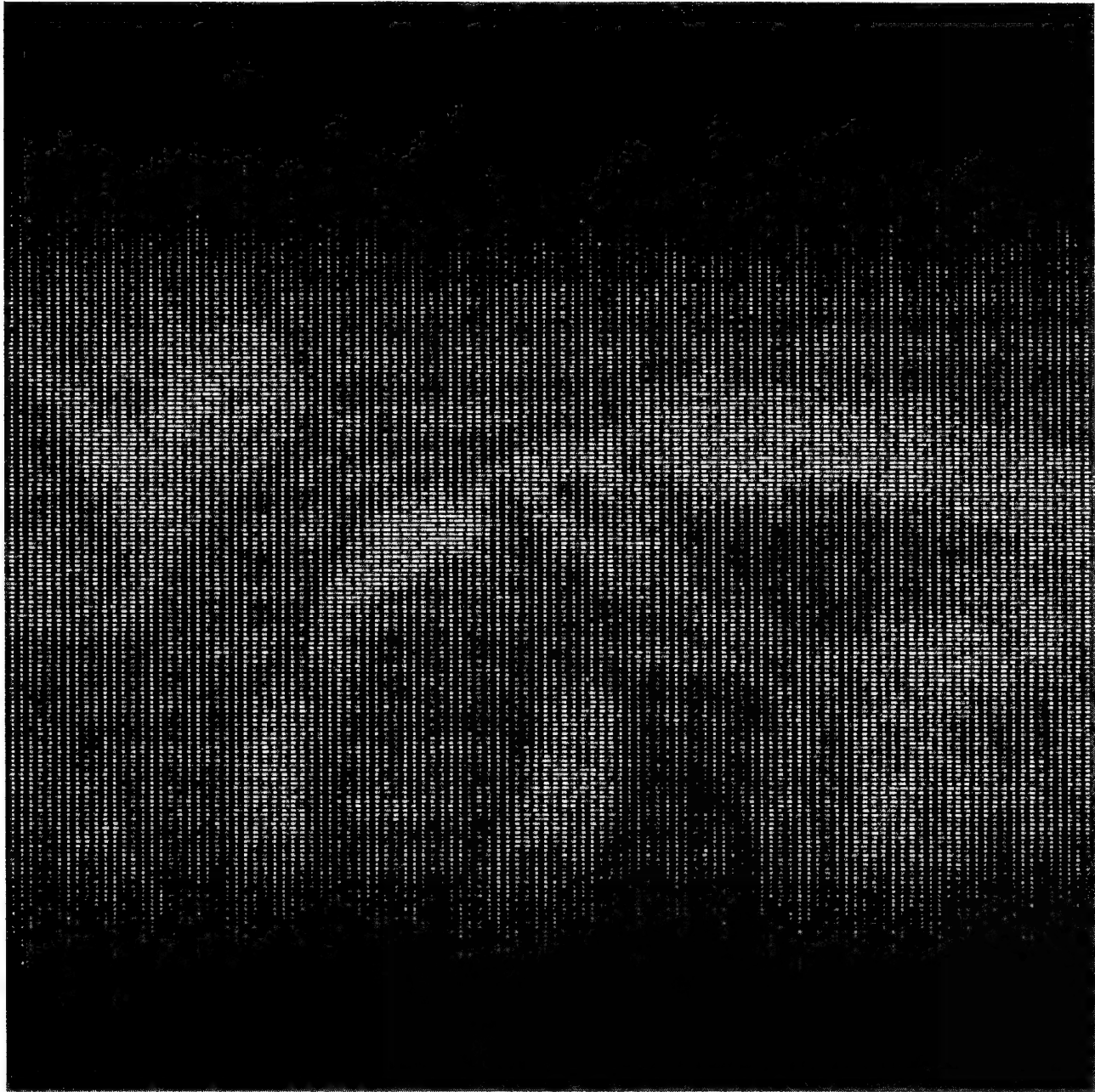
*** Lunch and Evening Functions by Invitation Only!**

Revised 7 January 2002

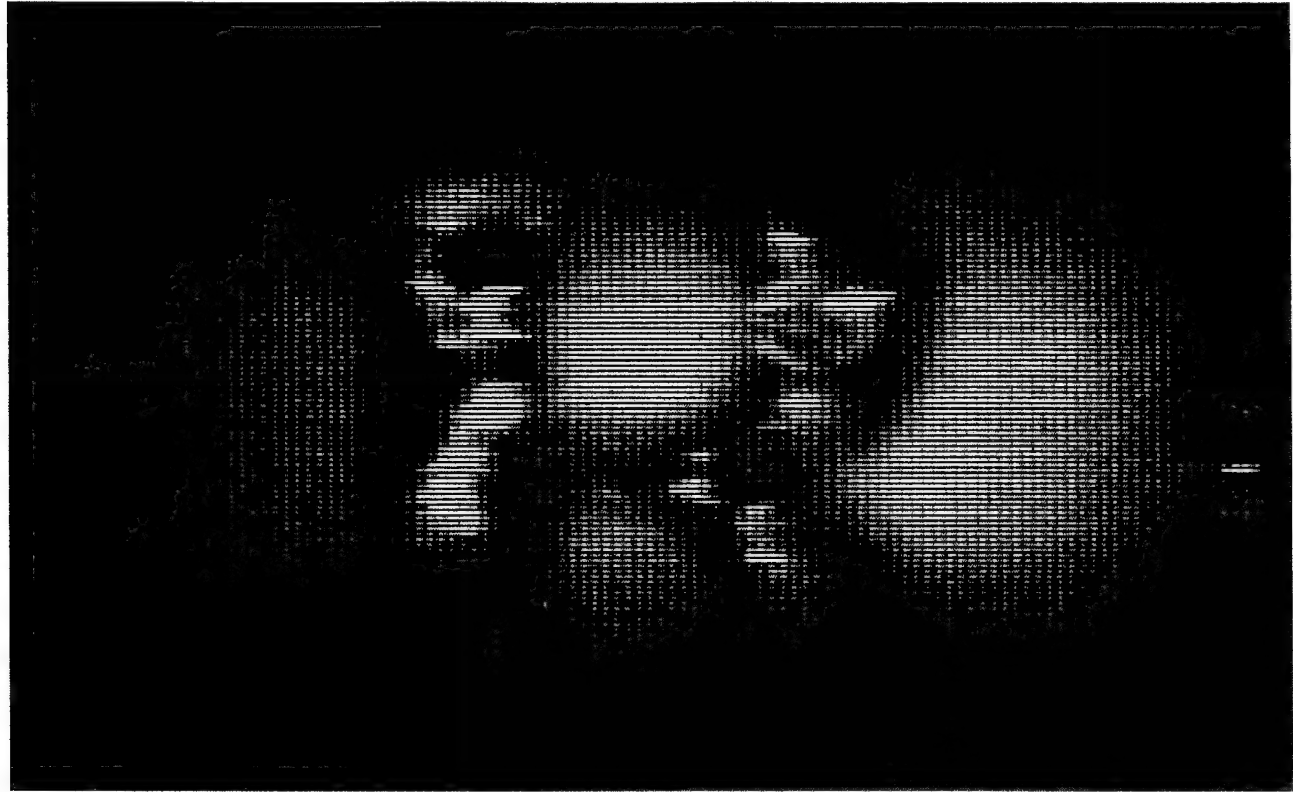
Schematic Diagram of Design 6 for the Remote Diagnosis of Retinal Damage



Results using a model eye target from Remote Diagnosis of Retinal Damage, Design 4



Results using a model eye target from Remote Diagnosis of Retinal Damage, Design 5



Results using a model eye target from Remote Diagnosis of Retinal Damage, Design 6



Project 5. Regeneration of Damaged Central Nervous System (CNS)
Investigator: Dr. Dong Feng Chen

Body:

Following injury, the postnatal mammalian optic nerve, like many other axonal pathways in the central nervous system (CNS), regenerates poorly.^{1,2} While this regenerative failure has long been attributed to extrinsic inhibitors in the environment of the mature brain,^{3,4} our recent research has demonstrated that there lacks an intrinsic component in mature CNS neurons to initiate axonal growth following injury.⁵ We have discovered that this intrinsic component is the anti-apoptotic protein Bcl-2.⁶ A prerequisite for successful regeneration of severed optic nerves in adult mammals is the activation of an intrinsic regenerative mechanism of retinal ganglion cell (RGC) axons, such as the induction of Bcl-2 expression. Since little is known about the molecular mechanisms and signals that regulate Bcl-2 expression, turning Bcl-2 expression on in postnatal RGCs remains a challenge.

Recent studies have shown that lithium, a simple monovalent cation that has been used safely in the treatment of human with manic and depressive episodes for more than 30 years, robustly increases the levels of Bcl-2 protein.⁷⁻⁹ RGCs have long been used as a model for the study of CNS neurons, but the effect of lithium on the retina has never been studied. We hypothesized that, if lithium induces Bcl-2 expression in neurons, it may not only prevent injury-induced degeneration of RGCs and other CNS neurons but may also promote the regeneration of their axons. Using RGC as a model of CNS neurons, we discovered:

1. Lithium induces Bcl-2 expression in the mouse retina

Using retinal explant cultures, we found that all of the cultures exposed to lithium revealed dose-dependent increases in Bcl-2 mRNA levels. The upregulation of Bcl-2 in the retina was observed when the concentration of lithium was as low as 0.2 mM, and it was 3-fold higher than that of non-treated culture when 1.0 mM of lithium was applied (Fig. 1). These results indicate that lithium acts on the retina to induce mRNA levels of Bcl-2 expression.

2. Lithium supports RGC survival

Using purified RGC cultures, we investigated whether lithium promoted directly RGCs' survival. RGCs were purified from P2 pups and cultured in the absence and presence of lithium (1.0 mM). In the absence of lithium, a majority of RGCs died after 5 days of incubation, and only $11.2 \pm 2.8\%$ survived (Fig. 2A, C). Addition of lithium promoted significantly the survival of RGCs by 2 fold ($P < 0.05$) and led to a $22.3 \pm 5.8\%$ survival rate of RGCs after 5 days of incubation (Fig. 3B, C). These results suggest that lithium acts directly on RGCs to exert a neuroprotective effect.

3. Lithium promotes RGC axon regeneration

To study the effect of lithium on RGC axon regeneration, we used a previously established model of retino-brain slice co-cultures, in which a retinal explant is placed directly against a

brain slice containing the target area of RGC axons, the superior colliculus. The co-culture model offers many advantages over those of the *in vivo* models as well as the cell culture system for studying drug activities in regulating CNS regeneration. Taking advantages of this model, we used tissues derived from postnatal day 2 mouse pups to prepare co-cultures (Fig. 3A). We found that, in the absence of lithium, cultured retinal explants sent 18 ± 7.4 neurites into brain slices, with an average length of 220 ± 43 μm ($n=8$). With increasing amounts of lithium (0.2-5.0 mM), the numbers and lengths of neurites that extended into brain slices increased in a dose-dependent manner. The effect of lithium peaked at 1.0 mM, with an average neurite number of 40 ± 9.8 and length of 780 ± 319 μm ($n=8$), yielding an approximate 3-fold increase in both the number and length of regenerating axons over those of untreated controls. In previous studies,¹⁰ lithium has been shown to exert a toxic effect at concentrations higher than 3.5 mM. This was similar to significantly reduced neurite outgrowth we observed in co-culture preparations with LiCl's concentration greater than 5.0 mM. Thus, we conclude that lithium is able to support the regeneration of retinal axons at its established therapeutic concentrations (0.5 – 1.2 mM).

4. The Promotion of Regeneration by lithium is Bcl-2 Dependent

We noted a close correlation between the lithium-induced increase in Bcl-2 expression and the increase in the number of surviving RGCs and their axon regeneration, suggesting that regulation of Bcl-2 expression is at least one of the mechanisms through which lithium mediates RGC functions. To determine if Bcl-2 is an essential component of lithium-mediated RGC survival and axon regeneration, we studied genetically engineered mice that were either deficient in Bcl-2 function (knockout, ko) or overexpressed the Bcl-2 transgene (tg).

We first examined retino-brain slice co-cultures prepared from Bcl-2 ko mice to determine whether Bcl-2 is required for lithium-induced RGC functions. Cultures derived from Bcl-2 ko mice displayed much less vigorous axonal growth from retina into brain slices than did those derived from wild-type (wt) and/or heterozygous littermates (Fig. 4). There was a greater than 3-fold reduction in the number of regenerating axons in cultures prepared from Bcl-2 homozygous ko mice compared with those from wt and heterozygous littermate controls. Treatment with 1.0 mM lithium failed to promote retinal axon regeneration in cultures prepared from Bcl-2 ko mice, while it induced an approximate 2-fold increase in axon regeneration in cultures prepared from both wt and heterozygous mice (Fig. 4). These results indicate that Bcl-2 is an essential contributor to lithium-induced retinal axon regeneration.

To determine whether induction of Bcl-2 expression was the only factor contributing to the lithium-induced RGC axon regeneration, we next studied mice overexpressing Bcl-2. Consistent with our previous findings, cultures prepared from Bcl-2 tg mice without any treatment exhibited robust retinal axon regeneration in comparison to the cultures prepared from the wt littermates (Fig. 5). Overexpression of Bcl-2 stimulated more than a 4-fold increase in axon regeneration from the retina into the brain slices over those of wt controls. The addition of lithium (1.0 mM) to the cultures promoted RGC axon extension in cultures prepared from wt mice, but had no effect in cultures prepared from Bcl-2 tg mice. Taken together, we conclude that lithium mediates RGC survival and axon regeneration via induction of Bcl-2 expression.

Key Research Accomplishments:

- Lithium induces Bcl-2 expression in the mouse retina
- Lithium supports RGC survival
- Lithium promotes RGC axon regeneration
- The promotion of regeneration by lithium is Bcl-2 dependent

Reportable Outcomes:

Hu tang X, Wu D-Y, Chen G, Manji H, & Chen DF. Support of Retinal Ganglion Cell Survival and Axon Regeneration by Lithium via a Bcl-2-dependent Mechanism. (2002) *IOVS* (submitted).

Abstract and presentation

Chen DF. Toward the Cure of Brain and Optic Nerve Damage. TATRC's 2nd Annual principal Investigators' Review, 2002, Jan. 23. Newport Beach, CA.

Patent

Chen DF, Huang X, Manji H, & Chen G. Methods and compositions for stimulating axon regeneration and preventing neuronal cell degeneration. (pending).

Conclusions:

Our study shows that lithium, acting directly on RGCs, supports both neuronal survival and axon regeneration at its established therapeutic concentrations (0.5 – 1.2 mM). We further demonstrate that addition of lithium induces Bcl-2 mRNA levels in mouse retinas. Depletion or overexpression of Bcl-2 gene both eliminates the regenerative-promoting effect of lithium in culture, indicating an essential role for Bcl-2 in this process. These results suggest, for the first time, that lithium may be used as a therapeutic drug for treating retinal and optic nerve neurodegeneration, e.g., glaucoma and optic nerve neuritis, and conditions involving optic nerve damage and/or RGC loss. They also offer new clues toward a better understanding of the regulation of retinal and CNS regeneration. To achieve full regeneration of the severed optic nerve to the CNS by lithium, it may be essential to combine lithium treatment with other drugs that mediate induction of a permissive environment in the mature CNS.

References:

1. Quigley HA, Nickells RW, Kerrigan LA, et al. Retinal ganglion cell death in experimental glaucoma and after axotomy occurs by apoptosis. *Invest Ophthalmol Vis Sci*. 1995;36:774-786.
2. Rabacchi SA, Ensini M, Bonfanti L, et al. Nerve growth factor reduces apoptosis of axotomized retinal ganglion cells in the neonatal rat. *Neuroscience*. 1994;63:969-973.
3. Goldberg JL, Barres BA. The relationship between neuronal survival and regeneration. *Annu Rev Neurosci*. 2000;23:579-612.
4. Fournier AE, Strittmatter SM. Repulsive factors and axon regeneration in the CNS. *Curr Opin Neurobiol*. 2001;11:89-94.

5. Chen DF, Jhaveri S, Schneider GE. Intrinsic changes in developing retinal neurons result in regenerative failure of their axons. *Proc Natl Acad Sci U S A*. 1995;92:7287-7291.
6. Chen DF, Schneider GE, Martinou JC, et al. Bcl-2 promotes regeneration of severed axons in mammalian CNS. *Nature*. 1997;385:434-439.
7. Chen G, Huang LD, Jiang YM, et al. The mood-stabilizing agent valproate inhibits the activity of glycogen synthase kinase-3. *J Neurochem*. 1999;72:1327-1330.
8. Chen RW, Chuang DM. Long term lithium treatment suppresses p53 and Bax expression but increases Bcl-2 expression. A prominent role in neuroprotection against excitotoxicity. *J Biol Chem*. 1999;274:6039-6042.
9. Manji HK, Moore GJ, Rajkowska G, et al. Neuroplasticity and cellular resilience in mood disorders. *Mol Psychiatry*. 2000;5:578-593.
10. Mitchell PB. Therapeutic drug monitoring of psychotropic medications. *Br J Clin Pharmacol*. 2000;49:303-312.

Appendices:

Figure 1. Lithium (Li^+) induces endogenous Bcl-2 expression in the mouse retina in a dose-dependent manner. (A) Photomicrograph shows the representative results of 2 replicate experiments of quantitative RT-PCR assessing the mRNA levels of Bcl-2 and G3PDH, a house-keeping gene, from cultured mouse retinas that were treated with differing concentrations of lithium. Note the markedly increasing levels of Bcl-2 mRNA in contrast to the consistent G3PDH levels. (B) Bar chart indicates the quantitative analysis of Bcl-2 mRNA levels in relation to the levels of G3PDH by semi-quantitative reverse transcriptase-polymerase chain reaction.

Figure 2. Lithium (Li^+) supports RGC survival in culture. (A-B) Phase-contrast photomicrographs show isolated RGCs in culture in the presence (A) and absence (B) of LiCl (1 mM). Arrows indicate surviving RGCs. Note increasing number of survival RGCs in the lithium-treated culture in comparison with that of untreated. (C) Bar graph illustrates quantitative result of RGC survival in the absence and presence of lithium following 5 days of incubation. Percent of RGC survival was determined by dividing the number of surviving RGCs, counted at the 5th day of culturing, by the number of RGCs originally plated. Data are presented as means \pm S.D. (*p <0.05). Scale Bar = 50 mM.

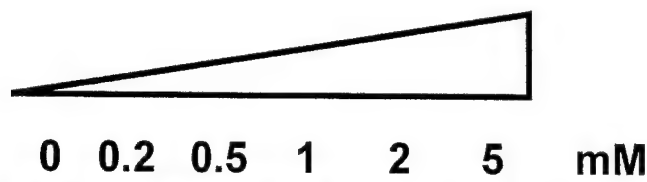
Figure 3. Lithium (Li^+) promotes RGC axon regeneration in a dose-dependent manner in culture. (A) Epifluorescence photomicrographs of representative retino-brain slice co-cultures in the absence and presence of LiCl. Regenerating axons were labeled by placing DiI into retinal explants and visualized under a fluorescence microscope. Arrows point to the labeled axons growing into the brain slices. (B-C) Bar graphs show the dose response curve of lithium on axon regeneration. (B) indicates the numbers of labeled axons extending into the brain slices. (C) indicates quantification for the longest distances of axon regeneration into the brain slices, measured from the interfaces of the retinal explants and brain slices. (* p<0.05 over control).

Figure 4. The regeneration-promoting effect of lithium (Li^+) requires Bcl-2 expression. Bar graphs present the number (A) and length (B) of regenerating axons in retino-brain slice co-cultures that were prepared from postnatal mice, either wild-type (+/+), Bcl-2 heterozygous (+/-), or Bcl-2 homozygous knockout (-/-). The cultures were prepared as

described and maintained in the absence or presence of 1 mM of LiCl. Error bars indicate S.D. (*p <0.05).

Figure 5. The regeneration-promoting effect of lithium (Li^+) is attenuated by overexpression of Bcl-2. Bar graphs present the number (A) and length (B) of regenerating axons recorded from retino-brain slice co-cultures prepared from tissues of wild-type mice (wt) or mice overexpressing Bcl-2 transgene (Bcl-2 tg). Error bars indicate S.D. (* p <0.05).

A

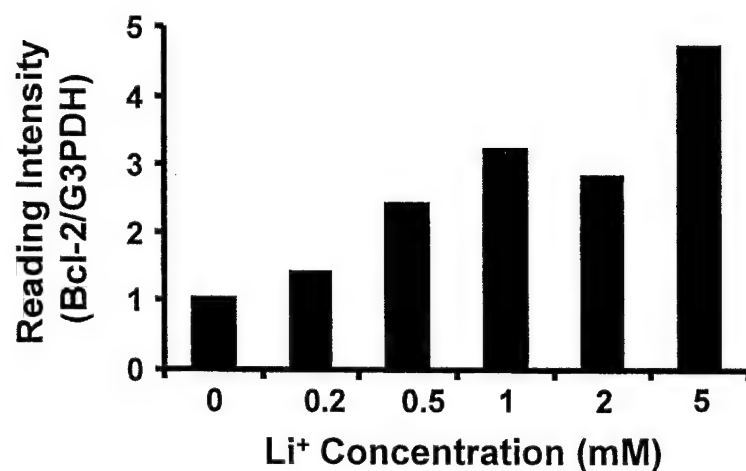


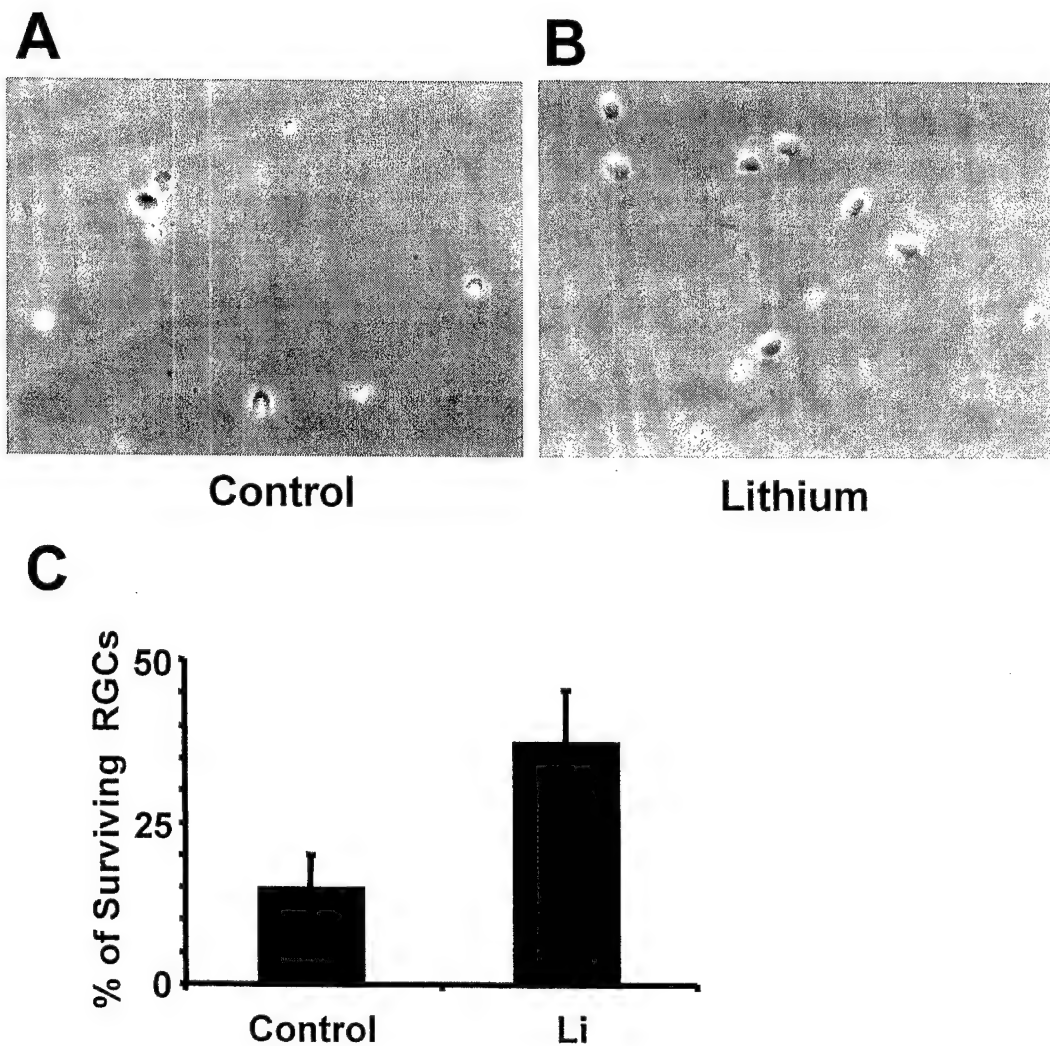
Bcl-2



G3PDH

B

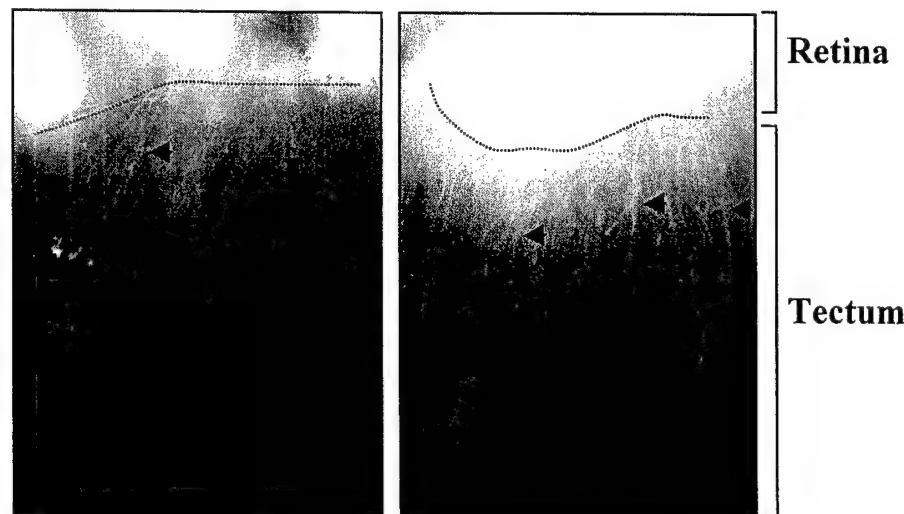




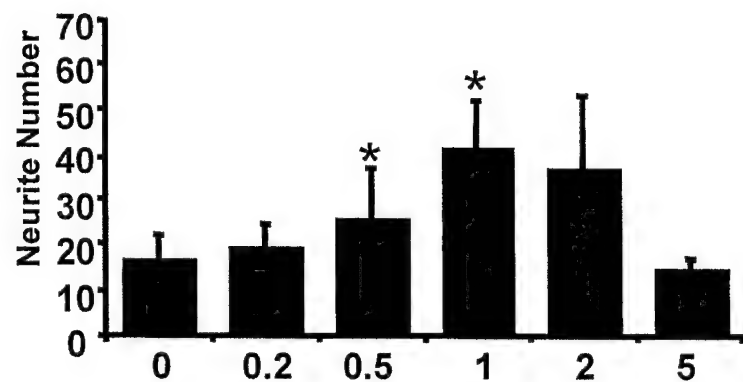
A

Control

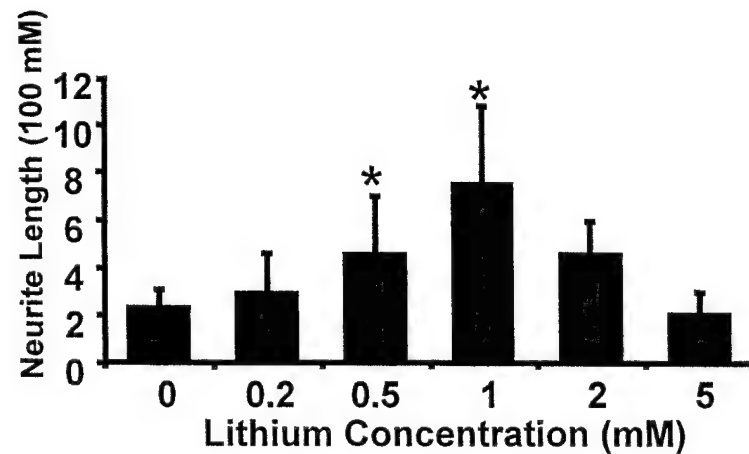
Li



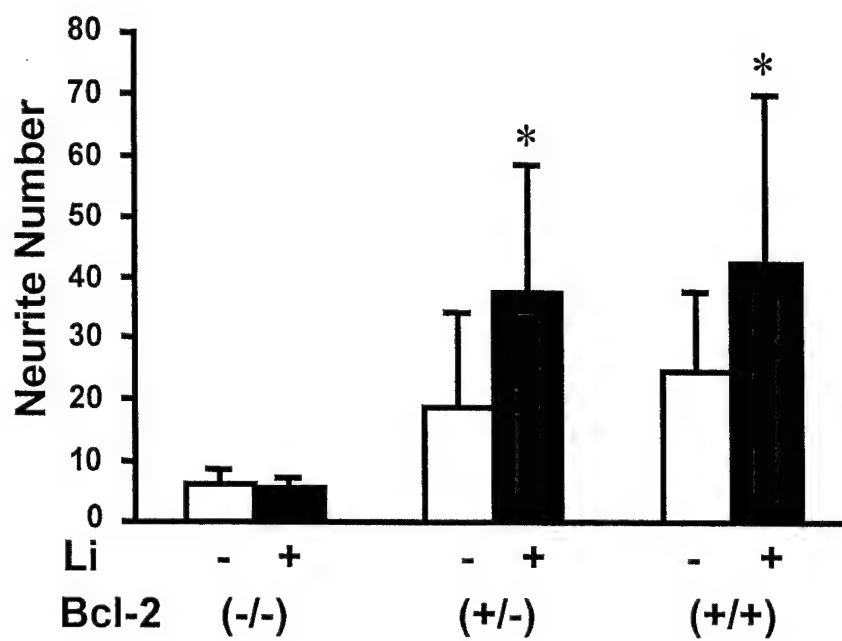
B



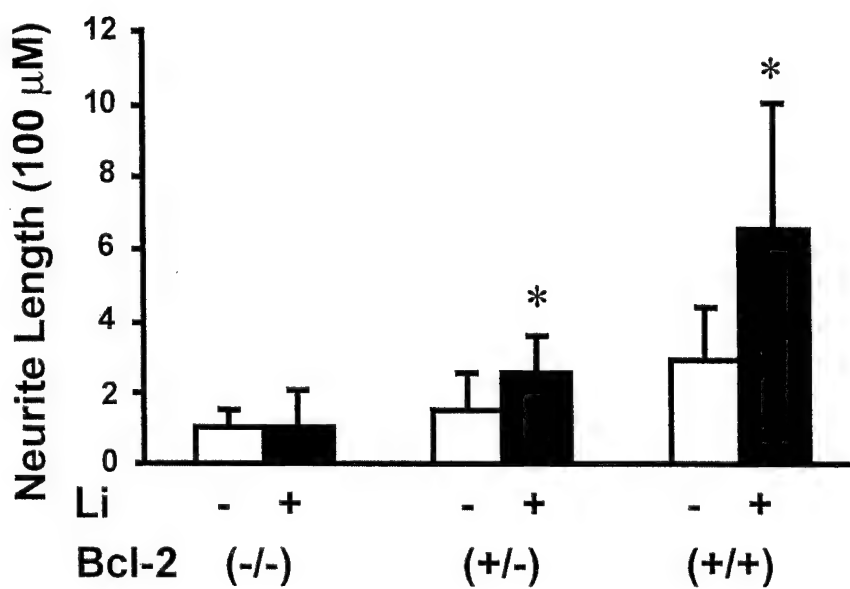
C



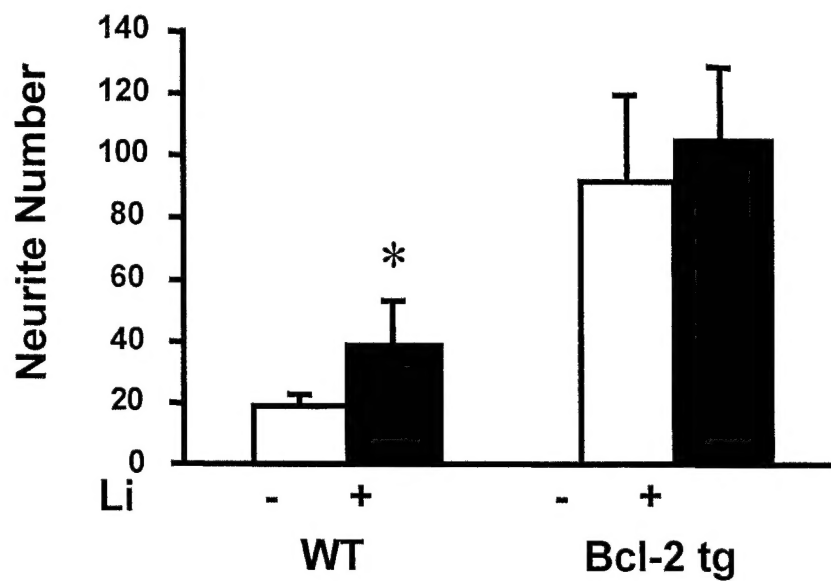
A



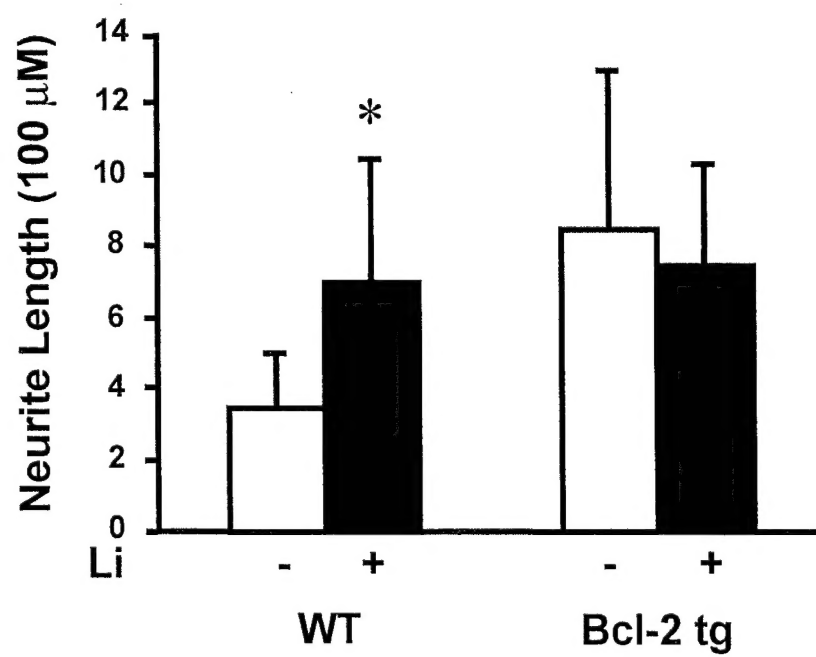
B



A



B



Project 6. Regulation of Angiogenesis: Role of VEGF in Adult
Investigator: Dr. Patricia D'Amore

Body:

Generation of mice with inducible expression of DN VEGFR2 in the endothelium

The goal of these studies is to be able to determine if VEGF signaling via VEGFR2 plays a role in the adult vasculature. We plan to accomplish this by generating mice in which a dominant negative (DN) form of VEGFR2 is inducibly expressed in the endothelium. To do this we have made two lines of mice: one in which the DN VEGFR2 is expressed as a transgene under the control of a tetracycline responsive element (pTRE-DN VEGFR2) and a second line in which the tetracycline activator is expressed in the endothelium. The pTRE-DN VEGFR2 transgenic mice will develop normally, because the TRE promoter is silent and no DN VEGFR2 will be expressed without rtTA and tetracycline/doxycycline.

In a second line of mice, the rtTA is knocked into the VEGFR2 locus. After successful targeting, expression of the rtTA cDNA will be under the control of the VEGFR2 promoter. Since the expression of rtTA would not affect normal development (Ewald et al., 1996; Kirby and Waldo, 1995; Mayford et al., 1996), the heterozygous VEGFR2^{+/−} rtTA knock-in mice will develop normally. Crossing these mice will give rise to a third line of mice in which the TRE promoter is silent, unless activated by rtTA (Gossen et al., 1995) and thus, the expression of DN VEGFR2 is controlled by rtTA.

Expression of DN VEGFR2 under the regulation of the tetracycline response element (TRE) in fibroblasts from transgenic mice

Two lines of mice carrying the pTRE-DN VEGFR2 have been generated. To demonstrate that the transgene is inducible in these mice, embryonic fibroblasts isolated from the transgenic embryos were transiently transfected with the pTET-ON vector (CMV-rtTA)(Clontech, Palo Alto, CA) that over-expresses the rtTA protein. Addition of doxycycline (1 µg/ml) for 24 hr led to the induction of high levels of DN VEGFR2 and the β-gal protein expression in the pTET-ON transfected fibroblasts. In the absence of doxycycline, however, neither DN VEGFR2 nor β-gal protein are detected in the pTET-ON transfected cells.

Demonstration of successful targeting in the homozygous VEGFR2-rtTA-KI targeted embryos

It has been previously reports that homozygous disruption of VEGFR2 is embryonic lethal (Shalaby et al., 1997). Therefore, if our attempts to target the rtTA to the VEGFR2 were successful, mice homozygous for the targeting should demonstrate embryonic lethality. We found that E 9.5 embryos, in which both copies of the VEGFR2 gene have been disrupted by the rtTA knock-in die around E10, and suffer from severe defects in vascular development. The heterozygous VEGFR2-rtTA-KI embryos were viable and developed to term with normal vascular development, similar to their wild-type littermates. This is the expected result and it is the heterozygous mice that are used in the breeding.

Assessment of DN VEGFR2 Expression

We have crossed the transgenic and knock-in mice described above and have fed these mice tetracycline/doxycycline at various time points (1 month, 2 months, 3 months of age) to induce the expression of DN VEGFR2. In spite of the results presented above, which document that the DN VEGFR2 is inducible and that the tet activator is correctly targeted, we did not observe significant expression of the DN VEGF2 in mice fed the doxycycline. We suspect that the weakness of the Flk-1 promoter and the structure of the Tet activator (leading to poor expression and instability) are the cause of this poor expression.

We are therefore using a transgene approach with the endothelial-specific PECAM-1 promoter (144-bp 5'-flanking) plus 8-kb enhancer (intron 2) to drive endothelial-specific rtTA expression. The PECAM-1 promoter plus enhancer (generously provided by Dr. Scott Baldwin, Children's Hospital of Philadelphia, PA), can confer consistent, high levels of endothelial-specific transgene (Lac Z) expression, both during embryonic development and in the adult (personal communication from Dr. Scott Baldwin and manuscript in preparation). Furthermore, unlike most of the other endothelial-specific promoters including Tie- 1 and 2, VEGFR1 and R2, which have been reported to be downregulated in the adult animal, the PECAM-1 promoter plus enhancer confers consistently high levels of endothelial-specific expression through development and into adulthood. In addition, we have obtained a modified tet activator construct which has been mutated to optimize expression in mammalian cells (Urlinger et al., 2000). We are currently subcloning this rtTA cDNA into this PECAM-1 promoter plus enhancer construct, and will use the resulting PECAM-1+Enhancer-rtTA construct to generate transgenic mice using standard techniques. By crossing the resulting PECAM-1+Enhancer-rtTA transgenic mouse with the pTRE-DN VEGFR2 transgenic mouse, animals with endothelial-specific and tetracycline-inducible DN VEGFR2 expression will be generated.

Key Research Accomplishments:

- Generated three lines of transgenic mice that express dominant negative VEGFR2 under the control of a tetracycline (Tet) responsive promoter.
- Demonstrated that the DN VEGFR2 is inducible in cells isolated from the transgenic mice
- Generated a line of mice in which the Tet activator is "knocked into" the flk-1 locus.
- Demonstrated that the "knock-in" was successfully targeted.

Reportable Outcomes:

None.

Conclusions:

The transgenic portion of this project has been successfully completed. The "knock-in" mouse though technically successfully does not express the Tet activator at sufficiently high levels to induce the DN receptor. Another line of mice in which the PE-CAM promoter as a transgene drives the Tet activator is currently under construction. Crossing these two lines of transgenic mice will provide mice in which we can test whether VEGF signaling is required in the adult vasculature.

References:

- Ewald, D., Li, M., Efrat, S., Auer, G., Wall, R. J., Furth, P. A., and Hennighausen, L. (1996). Science 273, 1384-1386.
- Gossen, M., Freundlieb, S., Bender, G., Muller, G., Hillen, W., and Bujard, H. (1995). Science 268, 1766-1769.
- Kirby, M. L., and Waldo, K. L. (1995). Circ Res 77, 211-215.
- Mayford, M., Bach, M. E., Huang, Y. Y., Wang, L., Hawkins, R. D., and Kandel, E. R. (1996). Science 274, 1678-1683.
- Urlinger, S., Baron, U., Thellmann, M., Hasan, M. T., Bujard, H., and Hillen, W. (2000). Proc Natl Acad Sci U S A 97, 7963-8.

Appendices:

None.